KLUEVER, LAURITZ GERHARDUS

SELECTIVE APPLICATIONS OF SOLID-PHASE REACTORS IN FLOW INJECTION SYSTEMS

MSc UP 1998

Selective applications of solid-phase reactors in flow injection systems

by

Lauritz Gerhardus Kluever

Submitted in partial fulfillment of the requirements for the degree

MAGISTER SCIENTIAE

in the Faculty of Science

University of Pretoria

Pretoria

1998

Selective applications of solid-phase reactors in flow injection systems

by

Lauritz Gerhardus Kluever

Supervisor: Prof. J. F. van Staden

Department of Chemistry

University of Pretoria

Degree: Magister Scientiae

Synopsis

In the development and use of flow systems there is a continual challenge to not only get a particular method as sensitive as possible, but also to keep reagent consumption low while miniaturising the system. These factors affect the total running cost of a system, and are therefore important when designing a system for a particular purpose.

In this dissertation the use of solid-phase reactors in flow systems is evaluated. The aims in using these reactors are reagent reduction and system simplification. The first two chapters of the dissertation aim to give a broad background on flow injection analysis as

well as solid-phase reactors. The first application discussed is the determination of manganese(II) in mining effluent with a redox reactor. The second application is the determination of sulphide in dairy effluent with a precipitating reactor, while the third is the determination of iron(III) in ground water and multivitamin tablets with a complexing reactor.

All these reactors, with the possible exception of the precipitating reactor, reduce the reagent consumption that is typical of methods normally used. With regard to system simplification and miniaturisation, the reactors, again with exception of the precipitating reactor, succeed in meeting the aims set at the start of the study.

Selektiewe toepassings van vastetoestand reaktore in vloei-inspuitsisteme

deur

Lauritz Gerhardus Kluever

Studieleier: Prof. J. F. van Staden

Departement Chemie

Universiteit van Pretoria

Graad: Magister Scientiae

Samevatting

Met die ontwikkeling en gebruik van vloeisisteme is daar voortdurend die uitdaging om 'n metode nie net so sensititief moontlik te kry nie, maar ook om terselfdertyd reagensverbruik laag en die sisteem so eenvoudig moontlik te hou. Hierdie faktore beïnvloed die lopende koste van 'n sisteem en is dus belangrik as 'n sisteem vir 'n sekere doel ontwerp moet word.

In die verhandeling word die gebruik van vastetoestand reaktore in vloeisisteme bespreek. Die mikpunte vir die gebruik van sodanige reaktore is die vermindering in reagensverbruik en die vereenvoudiging van 'n sisteem. Die eerste twee hoofstukke van die verhandeling poog om 'n breë agtergrond oor vloei-inspuitanalise sowel as vastetoestandreaktore te gee. Die eerste toepassing wat bespreek word is die bepaling van mangaan(II) in myn-afloopwater met behulp van 'n redoksreaktor. Die tweede toepassing is die bepaling van sulfied in melkery-afloopwater met 'n presipiteringsreaktor, terwyl die derde die bepaling van yster(III) in grondwater en multivitamientablette is.

Al drie bogenoemde reaktore, met die moontlike uitsondering van die presipiteringsreaktor, verminder reagensverbruik effektief in vergelyking met metodes wat normaalweg gebruik word. In verband met sisteemvereenvoudiging en -verkleining het die reaktore, weereens met uitsondering van die presipiteringsreaktor, daarin geslaag om die mikpunte wat gestel is, te bereik.

Bedankings

- My Hemelse Vader, want sonder Hom is ek niks.
- Amour, vir liefde, geduld en al daardie mooi dinge.
- My gesin, vir ondersteuning.
- My vriende, vir belangstelling.
- My medestudente, vir hulp.
- My studieleier, vir motivering.
- Niel, vir baie goeie idees.

Table of contents

Chapter 2 : Solid-phase reactors

Chapter 3 : Determination of manganese(II) in natural water and effluent streams using a solid-phase lead(IV)dioxide reactor

Chapter 4 : The determination of sulphide in effluent streams using a solid-phase lead(II)chromate reactor incorporated into a flow system

Chapter 6 : Final conclusions

CHAPTER 1

Flow-injection analysis: Background and theory

1.1 Introduction

Flow-injection analysis is an analytical technique that has been known in its current form from 1975 [1]. One of the earlier workers contributing toward the evolution of FIA is Leonard Skeggs, with his legendary 'AutoAnalyzer' that was introduced to the analytical community in 1957 [2]. This system was an example of a continuous flow analysis, or CFA technique, which aimed to automate sample treatment and -manipulation. This was done for better repeatability of analyses and less contamination, which are drawbacks of manual methods. The system worked on the principle of samples being aspirated into a continuously flowing carrier stream, with air bubbles inserted between the sample plugs to avoid cross-contamination and minimise dispersion of the sample plug. This system unfortunately required a debubbler before the detector, as bubbles could not be tolerated during the detection step. Later workers included Pungor *et al*, who described the first documented case where flow-injection was used in the form that it is known today [3].

It was only from 1970 to 1975 that the world's researchers began realizing and exploiting the full potential of flow-injection analysis. The true origin of the technique was a source

of some debate among the leading researchers in the field. Researchers like Ruzicka and Hansen in Denmark, who coined the name 'flow-injection analysis' used today [1], claimed the novelty of the technique, referring to features which distinguished it from existing techniques. Stewart *et al* maintained that the concept of FIA was latent in various existing analytical methods, such as chromatography, and that the eventual development of FIA was inevitable [4]. Mottola published an article in 1981 that considers all sides of the issue and comments objectively on the debate [5]. This author acknowledges the precedents of FIA methodology in other techniques, as well as the important work done by the pioneers of FIA.

When all factors are considered however, FIA remains a very exciting and versatile technique for analysis of almost any conceivable sample. The essential features that distinguish it from other techniques are:

- unsegmented flow
- sample injection
- controlled (partial) dispersion of the sample
- exact timing of detection under non-equilibrium conditions

1.2 Partial dispersion as a foundation for FIA

This concept is also the source of some confusion when the aspects of FIA are discussed. Ruzicka and Hansen state the term 'controlled dispersion' as one of the most important features of FIA. Valcárcel and Luque de Castro question this, stating that the term does

not distinguish FIA from CFA where the dispersion, albeit complete, is also controlled by the air bubbles [6]. They propose that the term 'partial dispersion' should be used when discussing the features of FIA.

1.2.1 Definition

Dispersion is defined by Ruzicka and Hansen [7] as the dilution a sample volume undergoes when injected into a flowing stream. In FIA the degree of dilution a sample undergoes is highly reproducible, because injection and detection are usually computer-controlled, reducing the chances of systematical errors. Furthermore, because detection takes place under non-equilibrium conditions it is critical to effect a repeatable injection of sample for each analysis.

1.2.2 Effect of dispersion on analytical parameters

The degree of dispersion of a sample influences two major analytical parameters in an FIA-system, namely peak height and return to baseline-time. These parameters are related to sensitivity and sample throughput respectively. Higher dispersion usually means lower sensitivity and lower sample throughput. Figure 1.1 shows a typical FIA-diagram with the different parameters.

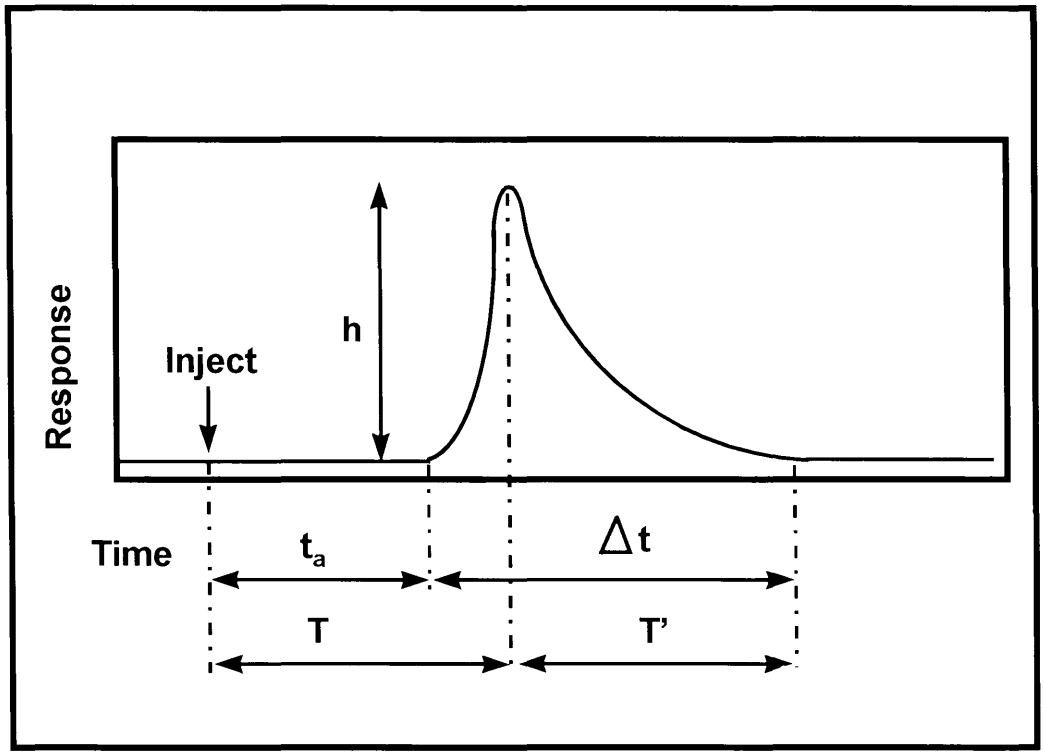

Figure 1.1: Diagram of a typical FIA-signal

h = peak height

t_a = travel time (time from injection to the first sign of the peak)

Δt = baseline-to-baseline time

T = residence time (time from injection to maximum signal)

T′ = return time (time from peak maximum to baseline)

As can be seen, the return time determines the sample throughput, because a new run can only be started once the signal has returned to the baseline. All these parameters are influenced by the conduits of the flow system, whether it be flow rate, sample volume, tube length or detector volume and -geometry. One can state that by controlling and

optimising the injection-, transport- and detection conduits, one is controlling the dispersion and subsequently the peak height (and area) as well as the time-related parameters.

1.2.3 Factors contributing toward dispersion

In FIA-systems there are two mechanisms contributing toward the dispersion of a sample plug, namely convective- and diffusional transport.

1.2.3.1 Convective transport

This type of transport occurs under laminar flow conditions (usually the case in flow-injection systems) and yields a well-defined parabolic sample profile. This is the case just after injection of the sample plug. Figure 1.2 shows an example of a sample plug under the above-mentioned conditions.

The direction of flow is indicated by the arrows. As can be seen, a concentration gradient is created, with a higher concentration of sample molecules at the front and center of the sample plug as well as at the back and sides. This gradient gives rise to a second factor contributing toward dispersion, which is described below

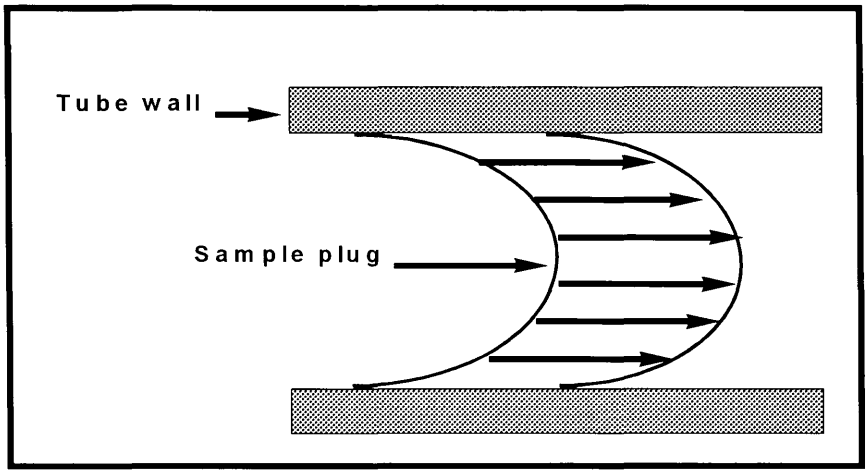

Figure 1.2: Diagram of a sample plug under laminar flow conditions

1.2.3.2 Diffusional transport

This type of transport occurs as a result of the concentration gradient created by the molecules at the tube walls moving slower than those at the center of the tube. The sample molecules at the front and center of the tube then tend to diffuse to the side of the tube. Likewise, the molecules at the back and sides of the tube tend to diffuse toward the center. This phenomenon is called radial diffusion and is illustrated in Figure 1.3.

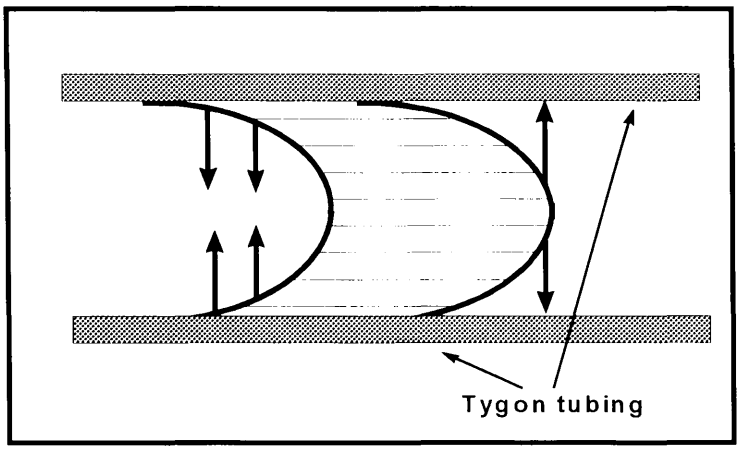

Figure 1.3: Diagram of a sample plug showing radial diffusion

Axial diffusion also takes place at the front as well as the back of the sample plug. This is shown in Figure 1.4.

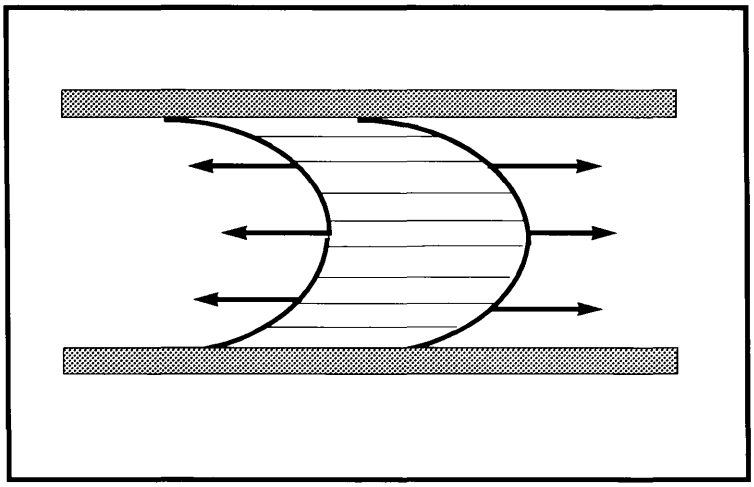

Figure 1.4: Diagram showing axial diffusion

1.2.4 Theoretical models for dispersion

A number of theoretical models have been proposed to describe or predict the dispersion of a sample plug in a flow system, but the one that best succeeds in doing this by taking into account the convective as well as the diffusional transport is the following:

$$D\left(\frac{\partial^2 C}{\partial \ell^2} + \frac{\partial^2 C}{\partial r^2} + \frac{1}{r}\frac{\partial C}{\partial r}\right) = \frac{\partial C}{\partial t} + u_0\left(1 - \frac{r^2}{R^2}\right)\frac{\partial C}{\partial \ell} \qquad (1.1)$$

where D denotes the dispersion coefficient, C the concentration, r the partial tube radius, ℓ the tube length, R the total tube radius and u_0 the linear flow rate [6].

The term at the left of equation 1.1 corresponds to diffusional transport, both axial and radial. The first term on the right of the equation accounts for the build-up of matter, while the second term accounts for convective transport.

This equation goes some way toward describing the dispersion and resultant analytical signal, but there is some discrepancy between the predicted values and experimental data due to the effect of PTFE connectors and the shape of the flow cell, among others.

1.2.5 Practical definition of the dispersion

Ruzicka et al have devised a practical definition of dispersion with regard to the concentration of molecules in a sample at a given time [7].

The practical dispersion is defined as the following:

$$D = \frac{C_0}{C} \tag{1.2}$$

where D is the practical dispersion, C_0 the sample concentration without dispersion and C the sample concentration at any given point in the system. In most cases the dispersion is considered at the peak maximum, so equation 1.2 becomes:

$$D = \frac{C_0}{C_{max}} \tag{1.3}$$

As is evident from the above equation, the value for the dispersion always exceeds unity, as C_{max} will be less than C_0 after transport through the system. Because of the relationship between concentration and the observed signal i.e. peak height; peak area, equation 1.3 can be written as follows:

$$D = \frac{h_0}{h_{max}} \tag{1.4}$$

The dispersion of any given FIA-system can then be determined experimentally by simply recording the peak height in absence of dilution as well as recording the peak height for a normal sample analysis. Figure 1.5 shows how the peak height decreases as dispersion increases. As can be seen, the return time increases with increasing dispersion.

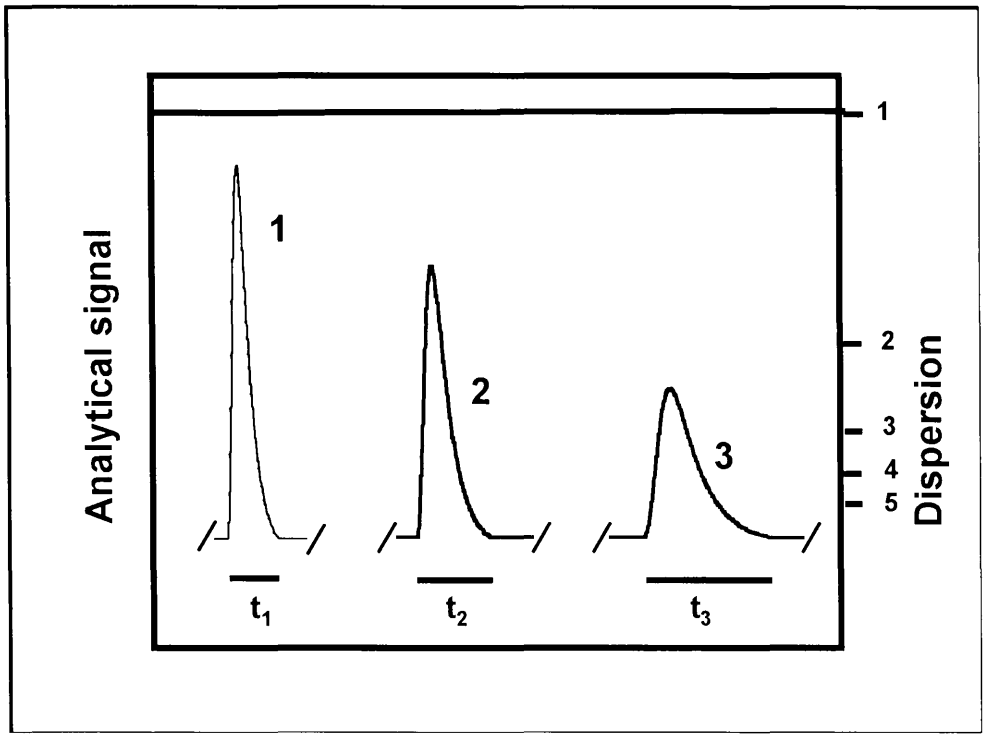

Figure 1.5: Diagram showing increasing return times with increasing dispersion

As can be seen, the peak heights decrease from peak number 1 to 3 as the dispersion, indicated on the right of the figure, increases. The return time for each peak is shown at the bottom of the peak. Evidently the return times also increase with increasing dispersion.

1.2.6 Influence of various factors on dispersion

The total dispersion in a flow-injection system is the result of mainly three factors, namely dispersion due to injection, transport and detection, as shown in equation 1.5.

$$D_{total} = D_{injection} + D_{transport} + D_{detection} \qquad (1.5)$$

where $D_{injection}$ refers mainly to dispersion occurring due to the sample volume and geometric aspects of the system.

$D_{transport}$ refers to the dispersion due to reactor geometry and the flow rate. (This is the most significant contribution to the total dispersion.)

and $D_{detector}$ refers to dispersion due to the detector geometry, which mostly concerns the shape of a flow-through cell.

1.2.6.1 Influence of the sample volume

In general an increase in the sample volume results in a decrease in the dispersion, with a subsequent rise in the return time T′. According to Ruzicka and Hansen [7] the dispersion is inversely proportional to the injected sample volume as in the following equation:

$$D = \frac{k}{V_i} \tag{1.6}$$

where k is a proportionality constant and V_i the injected volume.

1.2.6.2 Influence of flow rate

The flow rate can be related to the travel time t_a as well as the baseline-to-baseline time Δt. Both these relationships show an inverse proportionality between the flow rate and the time parameter. The baseline-to-baseline time should then decrease with increasing flow-rate, which indicates a decrease in dispersion.

1.2.6.3 Influence of the reactor shape

1.2.6.3.1 Straight tubes

This type of reactor represents the basic situation in a FIA-system and only the effect of varying tube length and diameter need be considered. In general, increasing tube length causes increasing dispersion, as does increasing tube diameter.

1.2.6.3.2 Coils

A coiled reactor has the effect of decreasing the dispersion normally experienced by a sample plug in a straight reactor of the same length, because of a radial-type flow created due to centrifugal forces around the axis of the reactor. This radial-type flow has the same effect as radial dispersion, discussed earlier.

1.2.6.3.3 Knotted reactors

Knotted reactors exhibit the same characteristics as coiled reactors, due to the fact that a knot can, in essence, be regarded as a very tight coil. Thus a knotted reactor should have a decreasing effect on the dispersion of a sample plug.

1.2.6.3.4 Packed reactors

The particle size of the reactor packing plays a vital role in the characteristics displayed by this type of reactor. Smaller particles tend to decrease the dispersion by increasing radial diffusion and are thus favoured above larger particles. The problem with this is that the reactor then has a much larger resistance to flow, increasing the pressure in the system up to a point where the type of pump normally used in FIA, namely peristaltic, can not handle the pressure. The researcher then has to consider using a high-pressure pump, like a piston-type pump. This elevates the cost of the system, but is worth implementing in some cases.

Packed reactors are very useful for a range of applications in FIA, especially where immobilised reagents are used. This is discussed in detail in the next chapter.

1.2.7 Influence of chemical kinetics on dispersion

In the previous discussions the effects of various factors have been discussed for a simple injection of a coloured substance into a carrier stream. No reaction kinetics has been studied or the additional effect on the dispersion of the sample plug investigated. The kinetics of a reaction can affect the dispersion in two ways, depending on whether some property of a reactant or that of a product is measured.

1.2.7.1 Reaction product measured

Some property of an increasing substance, namely the product, is measured, with the chemical kinetics causing a decrease in dispersion. An increasing rate constant causes decreased dispersion as well.

1.2.7.2 Reactant measured

When some property of a decreasing substance is measured, the chemical contribution is an increasing one. A higher rate constant results in higher dispersion.

1.2.8 Different degrees of dispersion

The extent of dispersion occurring in a given flow system is classified into three categories, namely limited, medium or large dispersion. They are classified according to the value obtained for the practical dispersion coefficient as defined in equation 1.4. Different applications can be found for these different degrees of dispersion.

1.2.8.1 Limited dispersion

This class of system typically has a dispersion coefficient of less than three (3) and is used to measure a parameter of the analyte without processes other than transport occurring. In order to keep the residence time as low as possible the flow rate has to be relatively high, typically above 2 $m\ell\ min^{-1}$, and in order to decrease the sample dispersion even more the sample volume should be rather large, usually one fifth of the reactor volume. The reactor in this case is a straight tube with a short length and small inner diameter.

1.2.8.2 Medium dispersion

These systems are designed to measure processes other than transport and have a dispersion coefficient of between three (3) and ten (10). The typical flow rates are lower than for the previous type of system and the reactors are longer, with larger diameters. Obviously sample frequency and sensitivity are lowered as well, due to increased dispersion.

1.2.8.3 Large dispersion

These systems have a high dispersion coefficient, typically higher than ten (10). A high degree of mixing is obtained between the sample and carrier, with equilibrium

being established in some cases. Systems with such a high degree of dispersion usually incorporate a mixing chamber or a very long reactor.

1.3 Essential FIA Components

A typical FIA-system consists of four (4) essential components:

- Propelling system
- Injection unit
- Reactor
- Detecting system

These different units are connected by Teflon connectors and Tygon tubing to form a flow-through system. The diameters and lengths of the connecting units can be varied for different applications.

1.3.1 Propelling systems

This is usually a peristaltic pump, which works on the base of a set of rollers forcing liquid through an elastic tube (Figure 1.6). Although these pumps are regularly used in FIA, they do have limitations with regard to the pumping of corrosive liquids like strong acids. This problem can be circumvented by the use of tubing resistant to corrosion, but such tubes are expensive and eventually show signs of corrosion as well. Peristaltic pumps also produce a pulsating flow, which

is more marked at higher flow rates. Their low cost and simplicity however, ensure their continued use in FIA.

Other types of pumps used include piston-driven pumps, either single or double, which are more expensive, but produce a smoother flow and can handle higher system pressures than peristaltic pumps.

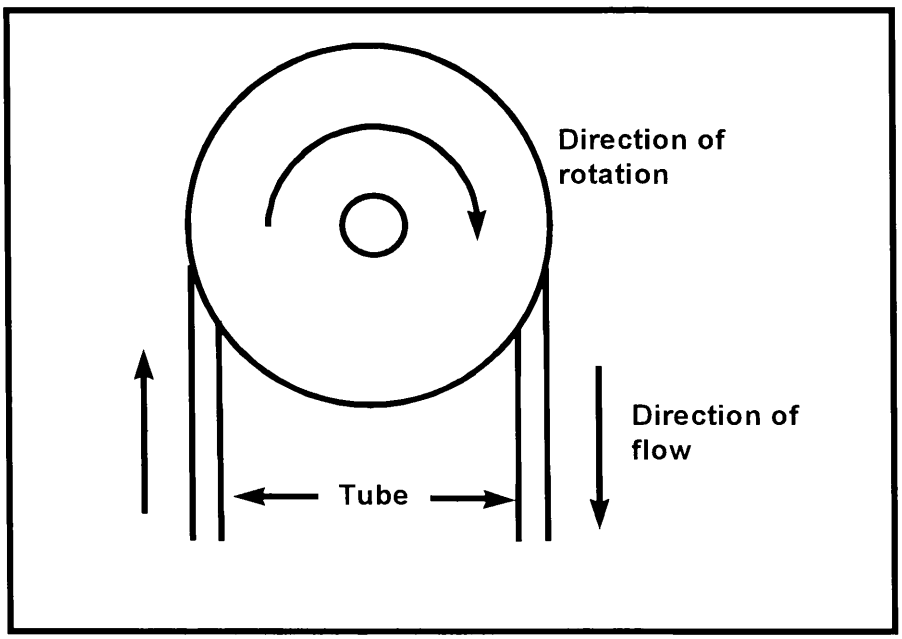

Figure 1.6: Working of a peristaltic pump

1.3.2 Injection system

The requirement of a sample injection device is to place a well-defined sample zone with an accurately measured volume into a carrier stream without disturbing the

flow of the carrier. The inserted sample plug should be reproducible for a large number of injections.

The most frequently used injection device in FIA is a rotary valve. This valve typically has six (6) to ten (10) ports which can be connected to different components of a system for single sample injection, double sample injection, dilution or preconcentration respectively. The valve consists of a number of different parts, of which the two most important are the rotor and the stator. The stator has a number of grooves on its surface that can be connected in different ways by the movement of the rotor. A valve usually has two positions, namely 'load' and 'inject'. The 'load'-position allows the sample plug to be filled and when the valve is switched to the 'inject'-position the sample plug is placed in the carrier stream. The valve arrangement for a single sample injection is shown in Fig.1.7.

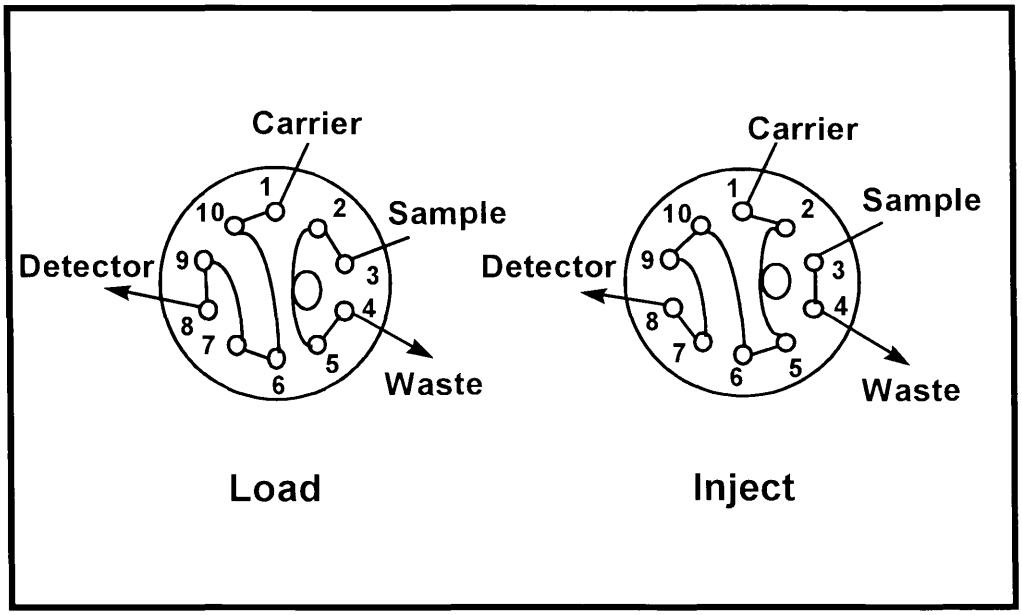

Figure 1.7: Valve arrangement for a single sample injection

Other types of injection systems used include proportional injectors and solenoid valves.

1.3.3 Reaction system

This part of the system can be made up of a number of different reactors. Reactors often used are straight tubes, coiled tubes, mixing chambers, packed reactors, open reactors or single bead string reactors. These reactors have been discussed in the section on partial dispersion in this chapter and are only mentioned here.

1.3.4 Detection system

According to Valcárcel and Luque de Castro a good detector should possess the following attributes:

- Low noise level
- Small dead volume
- Fast, linear response over a wide concentration range
- High sensitivity

A low noise level and high sensitivity of the system are essential to obtain a low detection limit, defined as the lowest concentration that can be assessed with a certain risk of error [6]. Some of the most commonly used FIA detectors are electrochemical detectors and optical detectors.

1.3.4.1 Electrochemical detectors

Detectors of this type can be classified into two categories, namely those whose response is based on properties of the solute or analyte and those whose response is based on properties of the bulk solution or carrier. Different types of detectors are given in Table 1.1.

Table 1.1: Types of electrochemical detectors used in FIA

Based on properties of the solution	Based on solute properties
Conductimetric	Amperometric
Capacitometric	Polarographic
	Coulometric
	Potentiometric

Detectors based on the properties of the analyte are highly sensitive and selective, but usually destructive to the analyte. Detectors whose response is based on the properties of the bulk solution, like conductometers, are not as sensitive as the previous type, but they are non-destructive in character which makes them ideal for intermediate monitoring.

1.3.4.1.1 Geometry of the detectors

Electrochemical detectors in FIA systems usually have one of three geometric designs, namely annular, wire or cascade. The different designs are shown in Figure 1.8, with the position of the electrode membrane indicated by the stars.

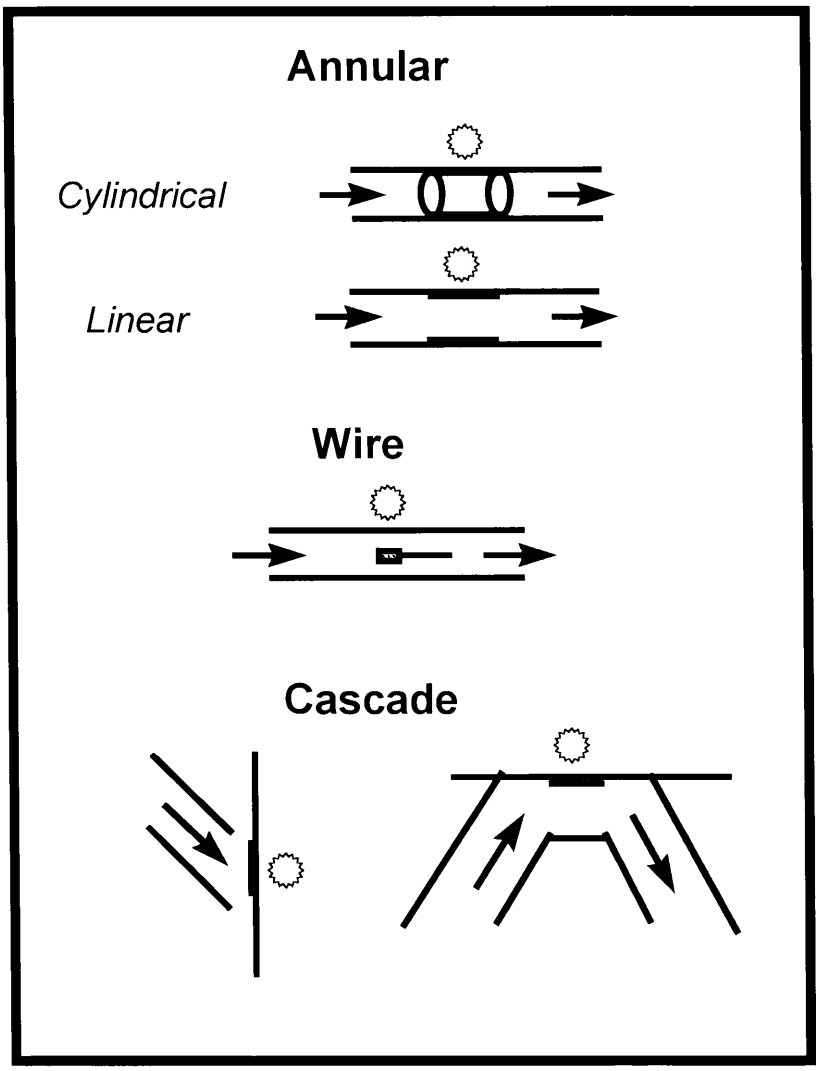

Figure 1.8: Typical shapes of electrochemical detectors

1.3.4.2 Optical detectors

1.3.4.2.1 Spectrophotometers

Due to the large number of species with optical properties that can be formed selectively in FIA-systems, this is the most popular detection technique. The ease

with which batch-type spectrophotometers can be converted for use in a flow system contributes to this popularity, as it requires little additional capital outlay for a normal cuvette to be replaced by a flow-through cell. Two types of flow-cells are used, the U-shaped cell and the Z-shaped cell, of which the U-shape is more popular. The design of a U-shaped cell is shown in Figure 1.9.

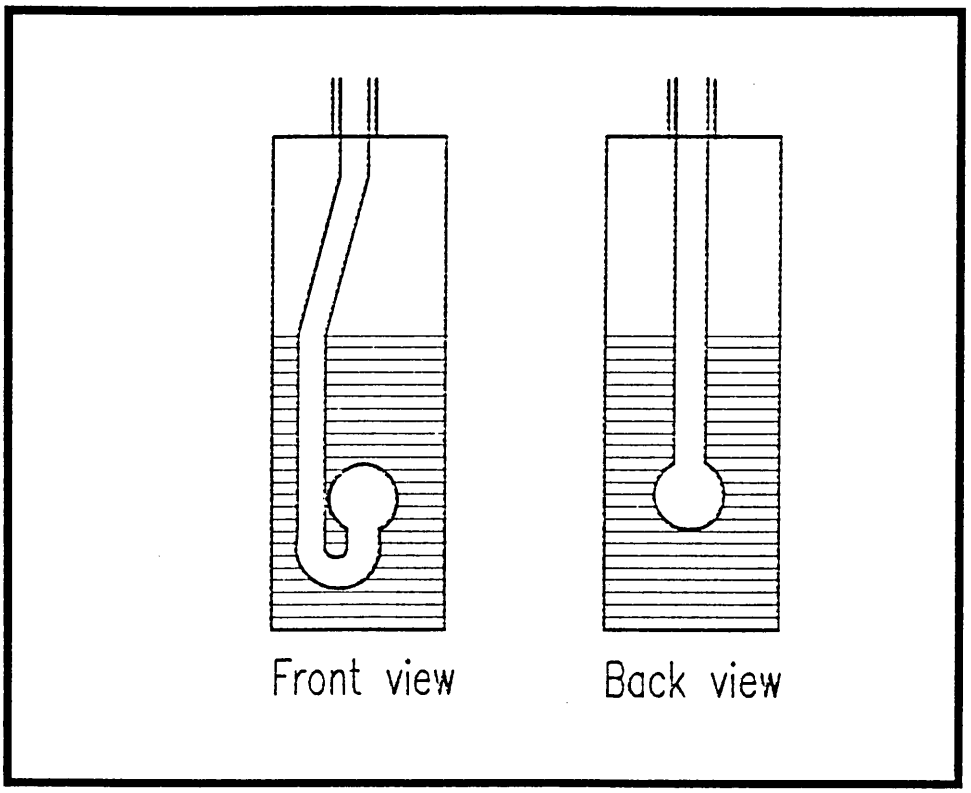

Figure 1.9: Typical design of a U-shaped cell

1.3.4.2.2 Atomic spectrometers

The ease with which a flow-injection system can be coupled to detectors using atomic absorption or emission as a sensing method, caused researchers to start exploiting the possibilities offered by this type of detector. The excellent sensitivity of graphite furnace AAS for instance, is very inviting as a detection device to an

FIA researcher working with very low levels of analyte. Likewise the versatility offered by ICP-AES offers the possibility of multi-analyte determination.

A factor that must be taken into consideration when coupling a flow system to a spectrometer is the maximum flow rate possible with the flow system. This flow rate must be compatible with the minimum required flow rate of the spectrometer so as not to starve or saturate the relevant flame or plasma. In the case of flame AAS which requires a high flow rate a make-up stream may be used if the optimum flow rate of the flow system is not high enough.

1.4 Aim of this work

The aim of this study done on flow-injection systems, incorporating solid-phase reactors, was to find an alternative flow injection method to analyse samples containing inorganic analytes. The goals were to minimise reagent consumption and miniaturise the flow system by introducing the reagent in the solid phase in a reactor. The different system configurations and applications possible with solid-phase reactors are discussed in chapter 2.

Chapters 3, 4 and 5 describe the experimental work done on three different systems, namely for the determination of manganese(II), sulphide and iron(III) respectively. For each system the following parameters were critically evaluated under optimum running conditions:

- Accuracy
- Precision

- Linear range
- Detection limit
- Sample interaction
- Interferences
- Sampling rate

The optimum running conditions were established by the univariate method, that is changing one particular system parameter to find the optimum while keeping the other parameters at a fixed value and then using the optimum value determined for the optimisation of the next parameter.

1.5 References

[1] J. Ruzicka and E. H. Hansen, **Anal. Chim. Acta, 78** (1975) 145.

[2] L. T. Skeggs, **Am. J. Pathol., 28** (1957) 311.

[3] E. Pungor, Z. Fehér and G. Nagy, **Anal. Chim. Acta, 51** (1970) 417.

[4] K. K. Stewart, **Talanta, 28** (1981) 789.

[5] H. A. Mottola, **Anal. Chem., 53** (1981) 1312A.

[6] M. Valcárcel and M. D. Luque-de-castro, **Flow-injection Analysis: Principles and Applications**, Horwood, Chicester,1987.

[7] J. Ruzicka and E. H. Hansen, **Flow Injection analysis**, John Wiley and sons, New York, 1981.

CHAPTER 2

Solid-phase reactors

2.1 Introduction

The use of reagents, particularly enzymes, in the solid phase has been known from the early part of the 20th century. These enzymes were immobilised on a variety of support materials for a number of reasons [1]. The enzymes were immobilised with specific features in mind, namely the multiple use of a single batch of enzymes, the ability to stop a reaction by removal of the enzyme, as well as analytical purposes such as predictable decay rates and elimination of reagent preparation. The use of these immobilised reagents thus offered a greater degree of control over the relevant reactions.

These types of heterogeneous reactions have been converted for use in flow-injection systems with some success [2,3]. In addition to the excellent analytical features already available with normal FIA-systems, systems which incorporate a solid-phase reactor offer further advantages with respect to miniaturisation. simplification and cost reduction.
Different types of immobilisation techniques for solid reagents are described in this chapter, along with the various shapes and types of reactors used. Various applications for the reactors are also discussed.

2.2 Modes of immobilisation

2.2.1 Natural

This type of immobilisation is used when the reagent is naturally very slightly soluble in the relevant medium and the particles are of approximately the desired size and consistency [5]. Large particles can also be ground to the desired size if necessary [4]. Usually one would want the particle as small as possible to have the maximum surface area available for reaction, but this may provide problems as the back-pressure resulting from usage of such small particles proves too much for normal peristaltic pumps to handle. This type of pump is mostly used in FIA to keep the total cost of a system relatively low. Piston-type pumps which can handle higher pressures can also be used, but this elevates the total cost. A compromise should be reached between the maximum surface area available with small particles and the effective back-pressure produced in the system.

2.2.2 Adsorption

This mode of immobilisation is mostly used when the reagent is a polar or even an ionic species [6]. The support for the polar reagent is then a corresponding polar compound such as silica or alumina and that for the ionic reagent a suitable ionic compound, such as an ion-exchange resin. The reagent is adsorbed onto the support material either by precipitation, or heating and evaporation of the solvent.

In chapter 3 the adsorption of lead(IV)dioxide onto silicagel is described for use in a redox reactor. There the immobilisation was achieved by oxidising an aqueous lead(II) solution with sodium hypochlorite, whereafter a solid precipitate was formed. This precipitate (PbO_2) immediately adsorbed onto the very polar silicagel present in the reaction mixture.

2.3.3 Entrapment

This method is often used for enzyme immobilisation when doing pharmaceutical analyses [7,8]. It involves making a slurry of the reagent to be immobilised, and physically 'trapping' or encapsulating it in a hardening polymer. Polyester resins are particularly useful in this regard. Martínez Calatayud and García Mateo [8] describe the use of a polyester resin to immobilise copper(II)carbonate. A copper(II)carbonate (25 g) slurry was stirred together with AL-100-A polyester resin and a small volume of the relevant catalyst added. This mixture was then stirred until it started to harden. The resin with the entrapped reagent ($CuCO_3$) could then be ground to the desired size and introduced into a reactor. This method for the immobilisation of solid reagents provides a great degree of control over the amount of immobilised reagent as well as the reagent to support ratio.

2.3 Types of reactors

Solid-phase reactors can be classified into two distinct groups, namely reactors in which a chemical reaction takes place to derivatise the analyte and reactors in which no

derivatising reaction takes place. The first group includes, among others, enzyme reactors while the second group consists mostly of reactors used for preconcentration.

2.3.1 Derivatising reactors

2.3.1.1 Redox reactors

This type of reactor employs a strong oxidising (for instance MnO_2 or PbO_2) [7,8] or reducing agent (for instance copperised cadmium) [3,9], which reacts with the analyte of importance to either render it in a suitable oxidation state for further reaction or for direct detection. The driving force for this type of reactor is the reduction or oxidation potential of the immobilised reagent. A typical reaction equation is:

$$Cd(s) + NO_3^-(aq) + H_2O(\ell) \Leftrightarrow Cd^{2+}(aq) + NO_2^-(aq) + 2OH^-(aq) \quad [E_0 = 0.402\ V]$$

This specific reaction is often used for the determination of nitrate. In this case the reaction is an intermediate one, as the formed nitrite still has to react with a diazonium salt to form an azo dye. The standard oxidation potential of the immobilised cadmium is 0.403 V and that of the nitrate -0.01 V. The nett standard reaction potential is then 0.402 V, as shown. Redox reactors are also used to prepare analytes for reaction with immobilised enzymes.

2.3.1.2 Complex-forming reactors

In this case the complexing agent, or ligand, is immobilised and reacts selectively with the metal analyte of importance when the latter moves through the reactor [10]. A typical reaction that may be used is:

$$Fe^{3+}(aq) + tiron^{2-}(s) \Leftrightarrow [Fe(tiron)]^{-}(aq)$$

In this case the tiron (1,2-dihydroxybezene-3,5-disulphonate) is in the reactor and reacts when the iron passes through. This reaction takes place in acidic medium. The resulting complex can then be detected spectrophotometrically at the wavelength of maximum absorption. This reactor works on the premise that the formation constant of the complex is high enough to overcome the interactive forces between the ligand and the support material, whether it be ionic or polar-polar interaction.

2.3.1.3 Precipitating reactors

This type of reactor is ideally suited for the indirect determination of anions. A very slightly soluble compound is immobilised in the reactor and reacts with the analyte to form an even less soluble compound, releasing the more soluble ion into the carrier stream [4]. This ion should then be in an easily detectable state, for

example chromate or dichromate, whose absorbance can be measured directly. A typical reaction that takes place is the following:

$$BaCrO_4(s) + SO_4^{2-}(aq) \Leftrightarrow BaSO_4(s) + CrO_4^{2-}(aq)$$

The solubility product of the analyte with different counter-ions plays an important role in developing a method incorporating this type of reactor. In this case the solubility product for $BaCrO_4$ ($K_{sp} = 2.4 \times 10^{-10}$) is higher than that for $BaSO_4$ ($K_{sp} = 1.1 \times 10^{-10}$) and the latter would thus precipitate, releasing the chromate into the carrier stream. The sulphate content of a sample can be indirectly determined in this fashion [4].

2.3.1.4 Enzyme reactors

As mentioned in the introduction of this chapter, the practice of immobilising enzymes for reaction in the solid phase has been known for quite a long time. Technology for enzyme-catalysed reactions for use in flow systems is also quite well known and these reactors comprise most of the solid-phase reactors currently in use in FIA [2,3,11,12]. The specificity of enzyme reactors ensure that there are few, if any, interferences for a given method and thus also reduce the enzyme consumption, which is an important factor when the high cost of enzymes are considered. A reaction consisting of four steps for the determination of inosine in human blood plasma is given below as an example of the simplicity and specificity

possible with immobilised enzyme reactors in flow systems. The reaction that takes place is the following:

$$\text{Inosine} \xrightarrow{\text{PNP}} \text{hypoxanthine} \xrightarrow{\text{XOD}} \text{xanthine} \xrightarrow{\text{XOD}} \text{uric acid} \xrightarrow{\text{UOD}} \text{allantoin}$$

where PNP = purine nucleocide phosphorylase

XOD = xanthine oxidase

and UOD = urate oxidase.

In the last three steps of the above reaction hydrogen peroxide is evolved, which then reacts with 3-(*p*-hydroxyphenyl)propionic acid (HPPA) in a horseradish peroxidase (HRP) mediated step to form a fluorophoric compound which can be detected fluorimetrically [2]. A diagram of the FIA-system is given in Figure 1.1.

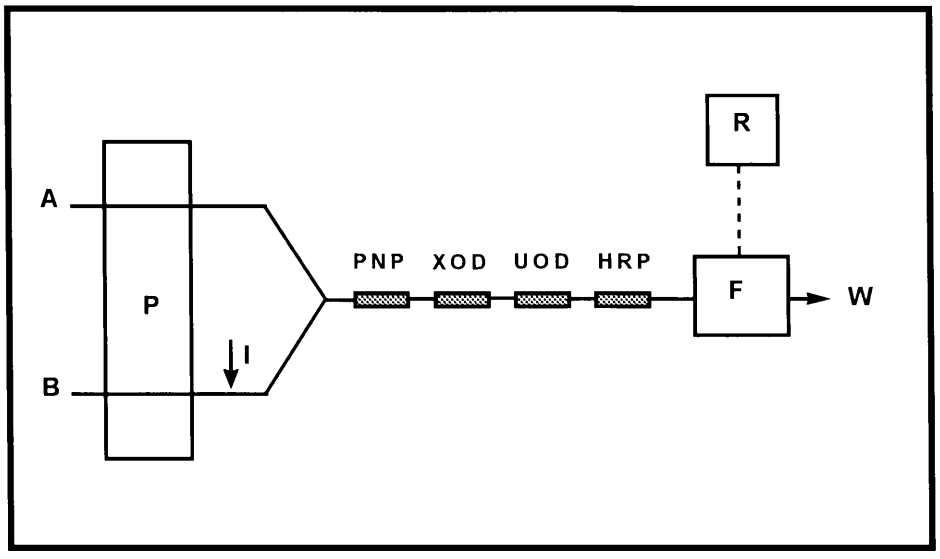

Figure 2.1 :Diagram of the system for determination of inosine

(where A = HPPA solution; B = carrier stream; P = peristaltic pump; I = point of sample injection; F = fluorescence detector, R = recorder and W = waste.)

2.3.2 Non-derivatising reactors

2.3.2.1 Adsorptive reactors

Preconcentration of metal ions is the most important use for this type of reactor, which consists of an adsorptive material like resins used for HPLC, packed in a conical container with both ends plugged with porous material. Enrichment factors of up to 50 have been achieved with the aid of conical reactors [13]. The conical shape of a preconcentration reactor ensures minimum dispersion of the retained analyte on elution, because retention takes place from the narrow end to the wider end, with elution taking place in the opposite direction. This elution of the analyte through a narrow aperture introduces a well-defined sample zone into the carrier stream. This type of reactor can be constructed with push-fit or threaded fittings for coupling to the transmission tubing, with each type of fitting having its own advantages and disadvantages with regard to ease of construction, long-term reliability, etc.

Another use for adsorptive reactors is as flow-through sensors for individual as well as multi-element determination [14,15]. These reactors are based on the

principle that the adsorptive material is placed in the flowcell of an FIA-system and retains a product formed in the system for absorbance or reflectance measuring. Multi-element determination is achieved by measuring absorption at different wavelengths with the aid of a diode-array spectrophotometer.

2.3.2.2 Reagent releaser reactors

These reactors have as their aim the decrease in dispersion of a sample plug by eliminating the merging point in a flow system usually necessary for reagent addition. The reagent is thus added from the solid phase directly into the carrier stream. This type of reactor can then be placed in the carrier stream before the injection point of the sample, where it will release the relevant reagent into the carrier stream. The system is also simplified, as the merging point, or points in the case of more than one reagent, usually requires Teflon connectors and extra tubing.

2.4 Shape of the reactor

2.4.1 Tubular

Most of the reactors in FIA are tubular or cylindrical in shape because of the flow-through nature of the method. The reagent, either immobilised on a support material or naturally insoluble, can be packed into the tube, column or cylinder with both ends of the reactor

closed off by glass wool or a similar porous, inert material. An example of a packed tubular reactor is given in Figure 2.2.

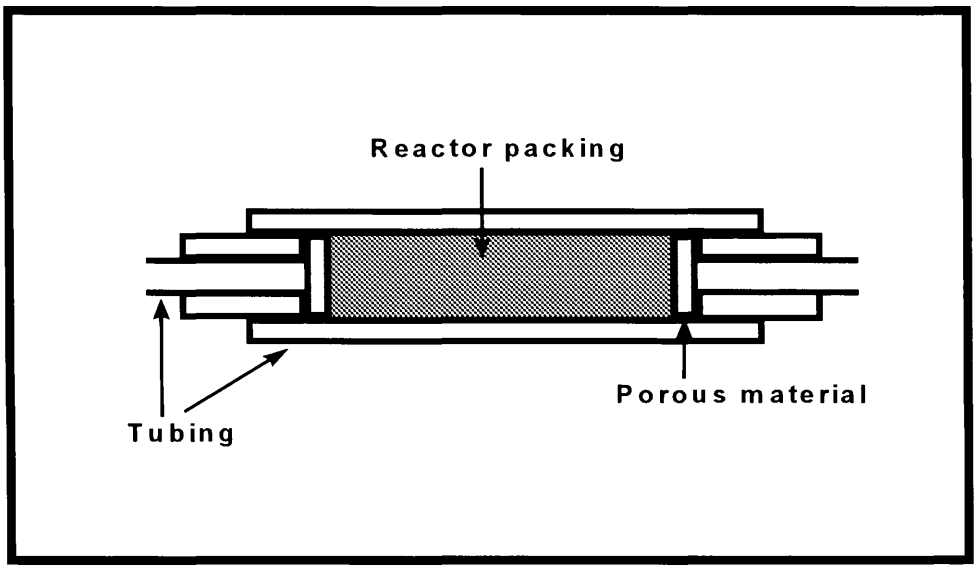

Figure 2.2: Design of a tubular packed reactor

As shown in Figure 2.3, another type of tubular reactor is also used, where the reagent is adsorbed or impregnated on or in the tube wall.

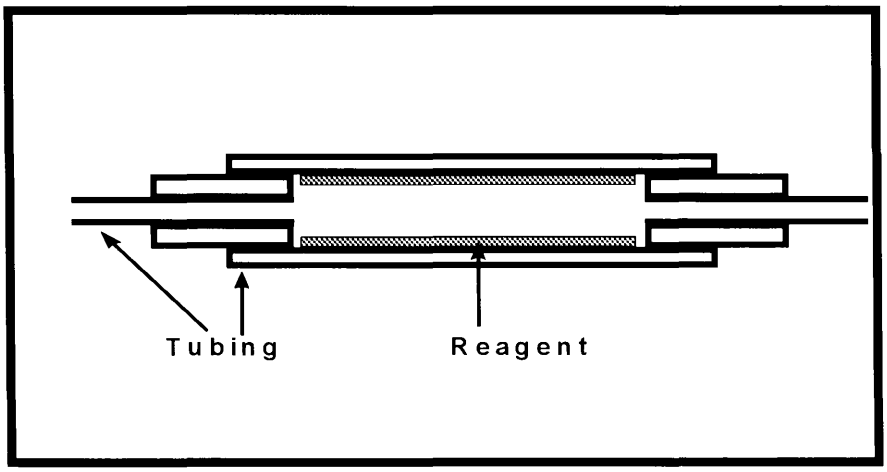

Figure 2.3: Design of an open tubular reactor

This type of reactor presents less resistance to flow and can thus be longer than packed reactors.

2.4.2 Conical

As mentioned previously in the section about the different types of reactors, the conical reactor shape is used when constructing preconcentration reactors [13]. A typical design of a push-fit reactor is shown in Figure 2.4.

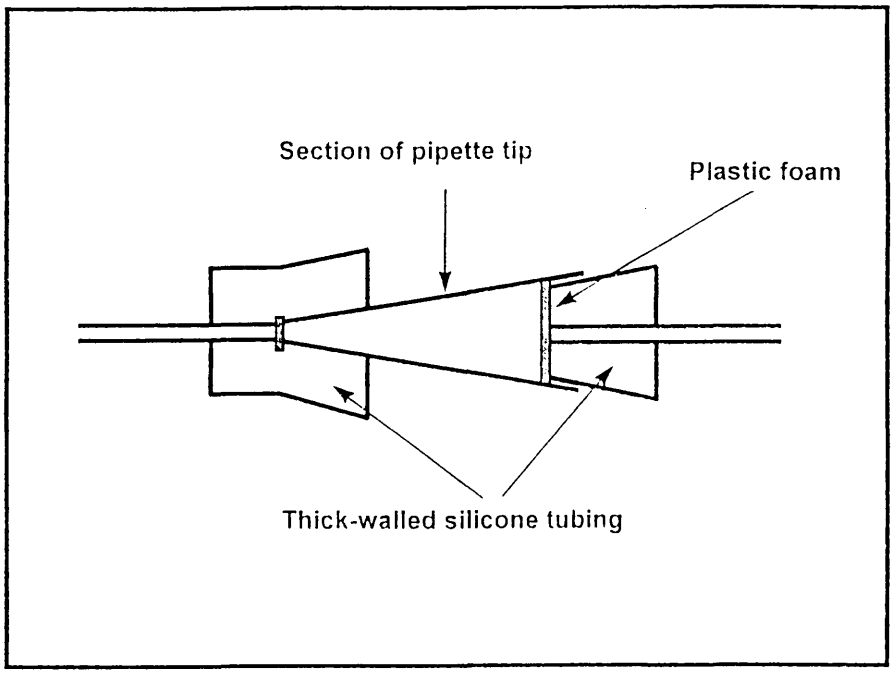

Figure 2.4: Design of a push-fit conical reactor

Both reactors with push-fit or threaded fittings for connection with valves and detectors perform satisfactorily, but with regard to long-term reliability and tolerance of high sample loading rates, reactors with threaded fittings are preferred over push-fit reactors. A reactor with threaded fittings is shown in Figure 2.5.

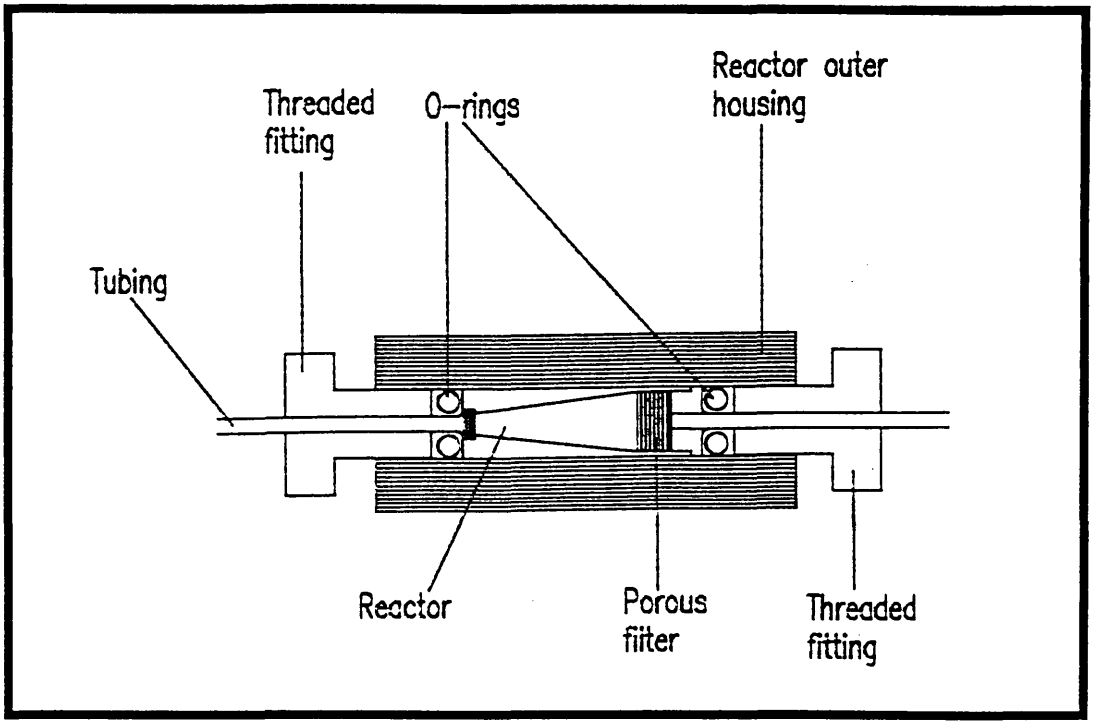

Figure 2.5: Conical reactor with threaded fittings

2.5 Position of reactor in the system

Solid-phase reactors can be put in various places in a flow system, depending on what the researcher or analyst wants to achieve with the system.

2.5.1 Before the injection valve

This location of the reactor is employed when there are impurities in either the carrier- or sample stream and the aim is to minimise or remove these impurities. The reactor in this case is usually an adsorptive reactor packed with C_{18} bonded silica for the removal of less

polar compounds or, to a lesser extent, silica or alumina for the removal of more polar compounds. A diagram showing the typical locations of a reactor in this mode is given in Figure 2.6.

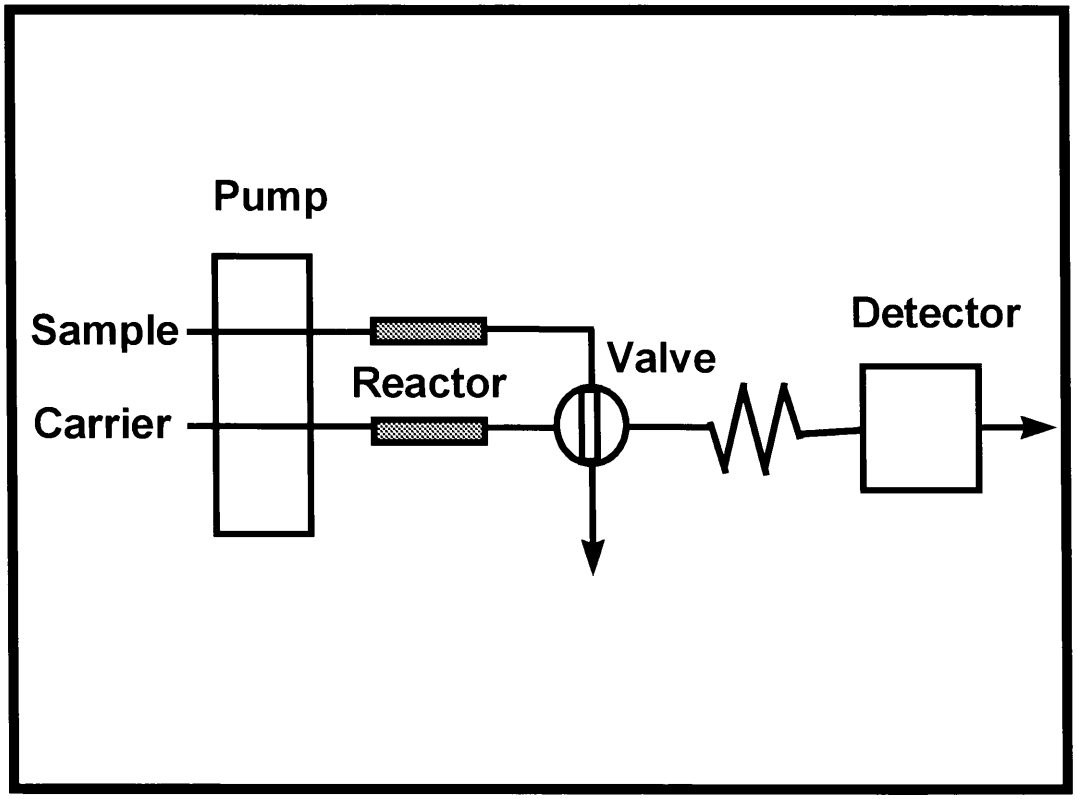

Figure 2.6: Prevalve positions for the reactor

Work has also been done with a reagent releasing reactor before the injection valve to minimise sample dispersion by eliminating the merging point for reagent addition, as discussed in the previous section [17].

2.5.2 In the injection system

This location is mostly used for preconcentration, with an adsorptive reactor placed in the sample loop of the injection system [18]. The retained analyte can then be eluted with a suitable eluent and pumped to the detector. A schematic diagram of this arrangement is given in Figure 2.7.

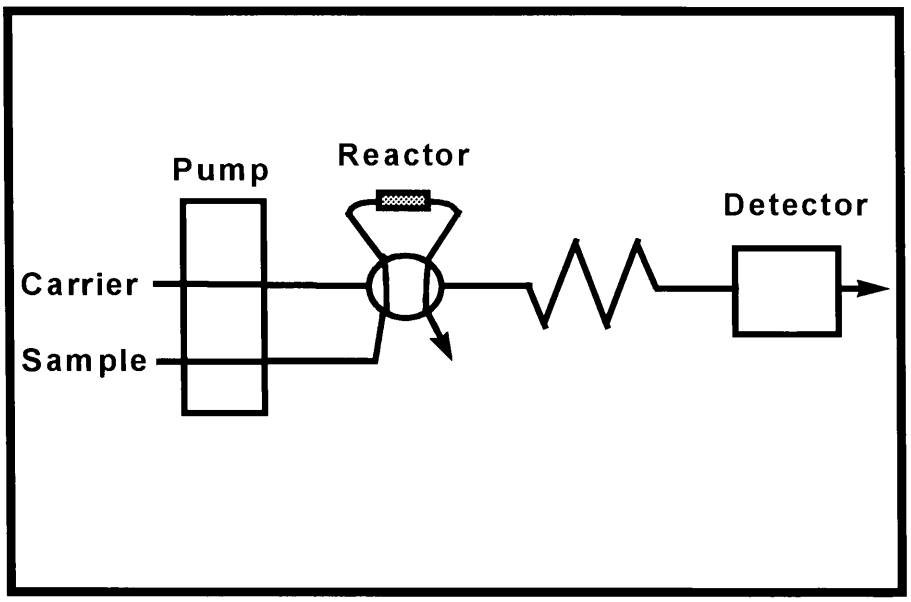

Figure 2.7: Diagram of reactor placed in the injection system

2.5.3 Between injection system and detector

This is the most common location employed for all types of solid-phase reactors. The sample is simply injected into the carrier stream and reacts with the relevant reagents as it passes through one or more reactors on its way to the detector. Any type of reactor can be used in this location for any application, whether it be enzymatic catalysis, oxidation,

preconcentration or complexation. A diagram of this system arrangement is given in Fig. 2.8.

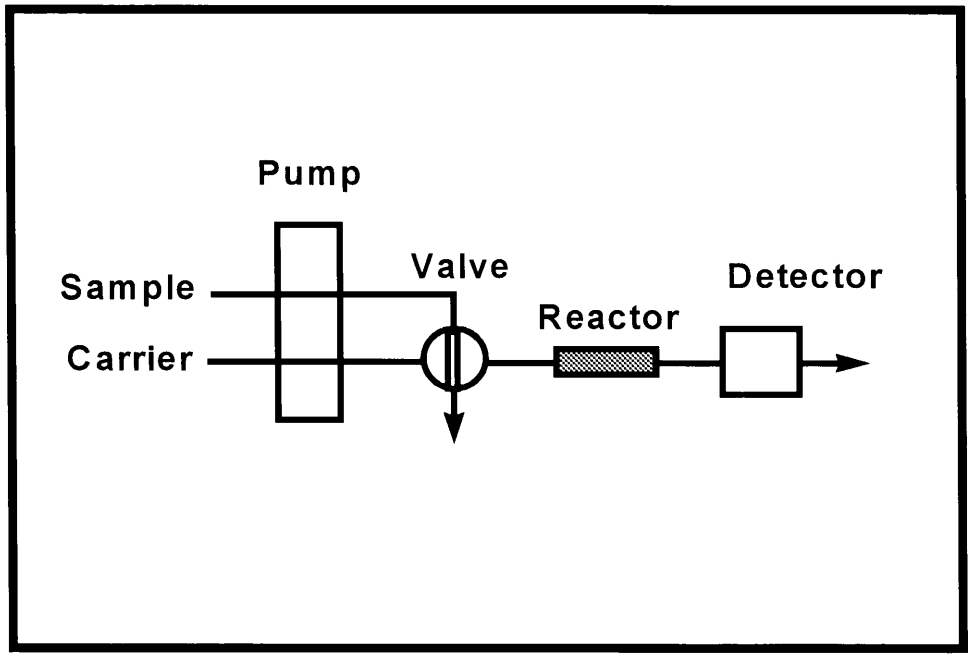

Figure 2.8: Diagram of the most common location for a solid-phase reactor

2.5.4 In the detector

This location for the reactor is used to integrate reaction and detection for a number of advantages, some of which are decreased dispersion of the sample zone, increased sensitivity and increased sample throughput. The system can be extremely small, as there is no need for an additional reaction unit or transport tubing. A diagram of this arrangement is shown in Figure 2.9.

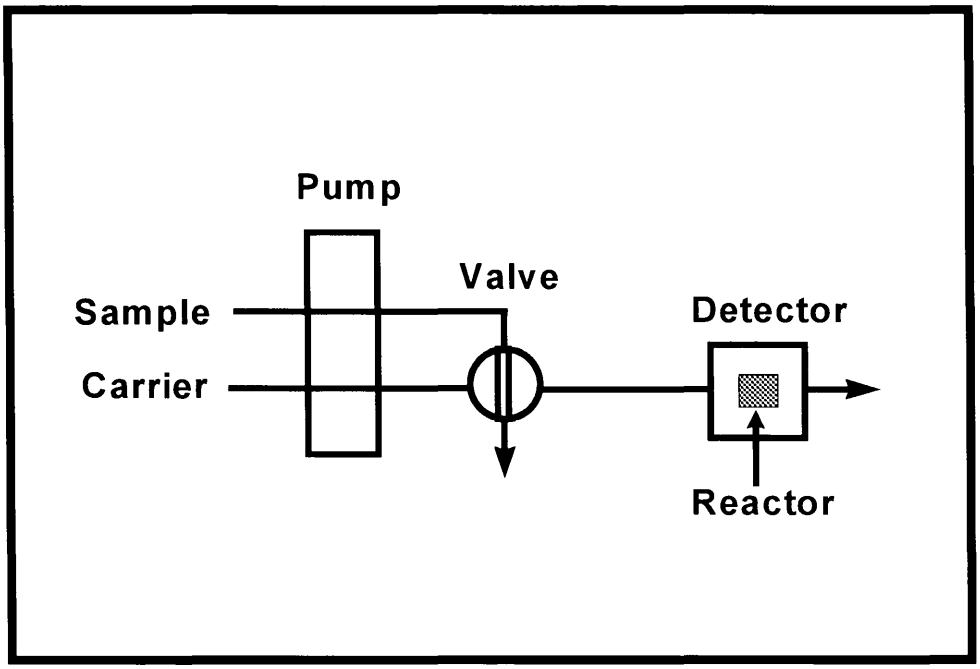

Figure 2.9: Diagram of system arrangement with reactor in detection unit

2.6 References

[1] R. A. Messing, **Immobilised enzymes for industrial reactors, Academic Press,** New York, 1975.

[2] K. Zaitsu, K. Yamagashi and Y. Okhura, **Chem. Pharm. Bull., 36** (1988) 4488.

[3] Y. Hayashi, K. Zaitsu and Y. Okhura, **Anal. Chim. Acta, 186** (1986) 131.

[4] A. Sakuragawa, S. Nakayama and T. Okutani, **Anal. Sci., 10** (1994) 77.

[5] R. Montero, M. Gallego and M. Valcárcel, **Anal. Chim. Acta, 234** (1990) 433.

[6] J. Martínez-Calatayud and S. Sagrado Vivez, **J. Pharm. Anal., 7** (1989) 1165.

[7] J. Martínez-Calatayud, J. V. García Mateo and L. Lahuerta Zamora, **Anal. Chim.**

Acta., 265 (1992) 81.

[8] J. Martínez-Calatayud and J. V. García Mateo, **Analytica Chimica Acta, 274** (1993) 275.

[9] T. Pérez-Ruiz, C. Martínez-Lozano, V. Tomás, J. Carpena, **Analyst (London), 117** (1992) 1025.

[10] J. F. van Staden and L. G. Kluever, **Anal. Chim. Acta., 350** (1997) 15.

[11] A. Fernández, J. Ruz, M. D. Luque de Castro and M. Valcárcel, **Clin. Chim. Acta, 148** (1985) 131.

[12] C. W. Bradberry and R. N. Adams, **Anal. Chem., 55** (1983) 2439.

[13] Z. Fang, **Flow-Injection Separation and Preconcentration**, VCH, Weinheim, 1993.

[14] D. Chen, M. D. Luque de Castro and M. Valcárcel, **Microchem. J., 44** (1991) 215.

[15] B. Fernández-Band, F. Lazaro, M. D. Luque de Castro and M. Valcárcel, **Anal. Chim. Acta, 229** (1990) 177.

[16] S. Tesfalidiet and K. Irgum, **Anal. Chem., 61** (1989) 2079.

[17] G. den Boef, **Anal. Chim. Acta, 216** (1989) 289.

[18] M. Karlsson, J. C. Persson and J. Möller, **Anal. Chim. Acta, 244** (1991) 109.

[19] B. A. Petersson, H. B. Anderssen and E. H. Hansen, **Anal. Lett., 20** (1987) 1977.

CHAPTER 3

Determination of manganese(II) in natural water and effluent streams using a solid-phase lead(IV)dioxide reactor.

3.1 Introduction

The determination of manganese in public and industrial waters is important, because it can cause discoloration of products, staining of clothes and reduction of pipeline carrying capacities due to encrustation. The most important cause for manganese found in ground- and natural waters is considered to be chemical erosion of the earth's crust [1]. Typical concentration ranges are in the order of 0.1 to 1.0 mg ℓ^{-1}. Usually the determination of manganese in these samples is done by laborious preconcentration techniques, but this requires a lot of sample handling. In South Africa the mining industry also contributes to the presence of manganese in natural waters and the concentrations may rise to a level of 200 mg ℓ^{-1} and even higher in certain effluent streams.

In past studies a number of methods for the determination of manganese have been reported, such as AAS, colorimetry, XRF spectrometry, ICP-AES, stripping

voltammetry and HPLC [2]. These methods usually require laborious sample preparation using large sample volumes and involve complicated procedures, which are time-consuming and expensive. In recent papers by Bowie *et al* [2] and Gaikwad *et al* [3] flow-injection analysis (FIA) is used with a chemiluminescence (CL) mode of detection. The advantage of using flow-injection over previously mentioned techniques is that it requires the least amount of sample handling accompanied by the minimum sample preparation steps involved.

Homogeneous reactions with the sample and reagent both in the liquid phase are used in most of the FIA manifolds [4 - 6]. This set-up may provide some disadvantages, particularly if the reagent is expensive, slightly soluble or only available in the solid form. Furthermore, one of the disadvantages of FIA is the relatively high reagent consumption per analysis. The use of solid-phase reactors incorporated into FIA manifolds may offer certain advantages. The advantages offered by solid-phase reactors over homogeneous systems have been discussed in comprehensive reviews [7,8] as well as chapter 2 of this thesis and all of them are not repeated here. However, some operational advantages of heterogeneous systems over homogeneous systems should be mentioned. The reagent consumption is greatly reduced and the system is simplified with fewer junctions for blending of reagent, sample- and carrier streams. In this system there is only one stream, namely the carrier, which flows through a reactor filled with the PbO_2 embedded on glass beads, or solid-phase reactor (SPR).

In this chapter the use of an FIA-system for the determination of manganese is described. The system is a modification of a method proposed by Rüter and Neidhart [1] in which manganese(II) is reacted with a strong oxidising agent, in this case PbO_2,

in the solid phase to produce the permanganate ion (MnO_4^-), which is determined spectrophotometrically.

According to Rüter and Neidhart [9,10], PbO_2 in nitric acid, along with sodium bismutate and potassium persulphate under the catalytic effect of silver salts are well-known agents for the oxidation of divalent manganese to manganese(VII).

The balanced equation for this reaction is:

$$2Mn^{2+}(aq) + 5PbO_2(s) + 4H^+(aq) \Leftrightarrow 2MnO_4^-(aq) + 5Pb^{2+}(aq) + 2H_2O(\ell)$$

The E_o-value for the oxidation of Mn^{2+} to MnO_4^- under standard conditions is -1.51 V and that for the reduction of PbO_2 to Pb^{2+} is 1.46 V. Under standard conditions the nett reaction potential would be -0.05 V and one would not expect a reaction. The conditions used in this study are far from standard, however, and these conditions are chosen so that the above reaction does occur. Factors like pH, catalytic effects and temperature are especially important in this regard, with decreased pH and increased temperature favouring the oxidation of manganese(II). This reaction is thus pH-dependent, and the oxidation of Mn^{2+} is accompanied by a rise in the pH of the solution that results in a decrease in the efficiency of the reaction. The reaction conditions are kept at an optimum by using an acidic carrier stream.

3.2 Experimental

3.2.1 Reagents and solutions

All reagents were prepared from analytical-reagent grade chemicals unless specified otherwise. All aqueous solutions were prepared with doubly distilled, deionised water from a ModuLAB Modupure water purification system (Continental Water Systems International). A stock standard manganese(II) solution containing 1000 mg ℓ^{-1} Mn^{2+} was prepared by dissolving 3.639 g of manganese(II)chloride tetrahydrate (Merck, pro analysi) and diluting to 1 litre with water. Working manganese(II) solutions in the range 1 to 50 mg ℓ^{-1} were prepared by appropriate dilution of the stock solution with 0.1 mol ℓ^{-1} HNO_3. These solutions were standardised with the aid of a flame atomic absorption spectrometer.

The carrier was prepared by dilution of 17 mℓ HNO_3 (55%, UNIVAR; SAARCHEM) with deionised water to a volume of 2 ℓ to give a final concentration of 0.1 mol ℓ^{-1}.

3.2.2 Instrumentation

The FIA system was constructed from the following components: a Cenco peristaltic pump operating at 10 rpm, a VICI 10 port 2-position sampling valve, a Thermomix temperature-controlled water bath (B. Braun; Germany), a Unicam 8625 UV-visible

spectrophotometer equipped with a Hellma flow-through cell (volume 80 $\mu\ell$) for absorbance measurements and a FlowTEK [11] software package.

3.2.3 Operation of the system

A schematic diagram of the flow-injection system is given in Fig.3.1.

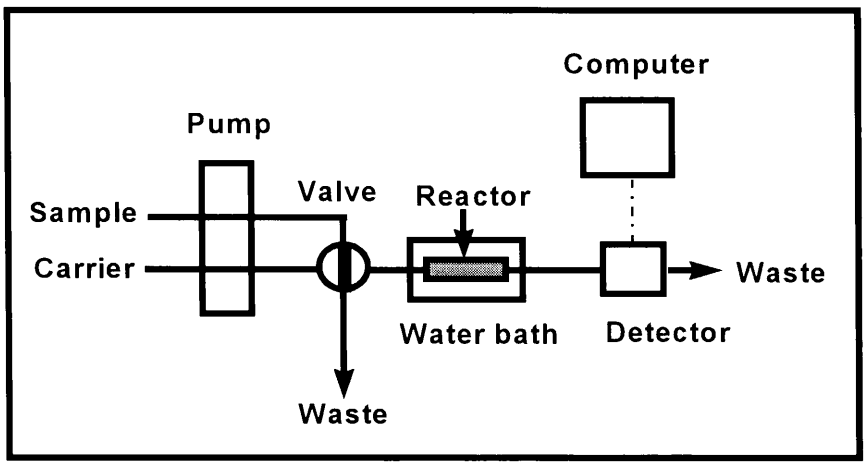

Figure 3.1: Diagram of the FIA system

The whole procedure, from sample injection to detection, data processing and storage was computer-controlled via the above-mentioned FIA-program, except the operation of the peristaltic pump and the waterbath, which had to be done manually.

The sample- and carrier streams were pumped through the manifold at flow speeds of 0.60 $m\ell\,min^{-1}$ and 2.00 $m\ell\,min^{-1}$ respectively. The injection valve was kept in the 'load' position for the first five seconds of every run, after which it was switched to the 'inject' position to place the sample plug into the carrier stream. The valve was kept in the 'inject' position for a further 75 seconds to ensure that all of the sample was flushed

out of the sample loop. This was followed by the switching of the valve to 'load' to fill the sample loop for the next run. After being placed in the carrier stream, the sample plug was pumped through the solid-phase reactor, which was immersed in the temperature-controlled water bath. From there it was pumped through the detector for measurements. The data obtained was converted to a response (arbitrary units) versus time graph and the maximum peak height was determined with and stored on a computer via the FlowTEK-program [11].

3.2.4 The solid-phase reactor

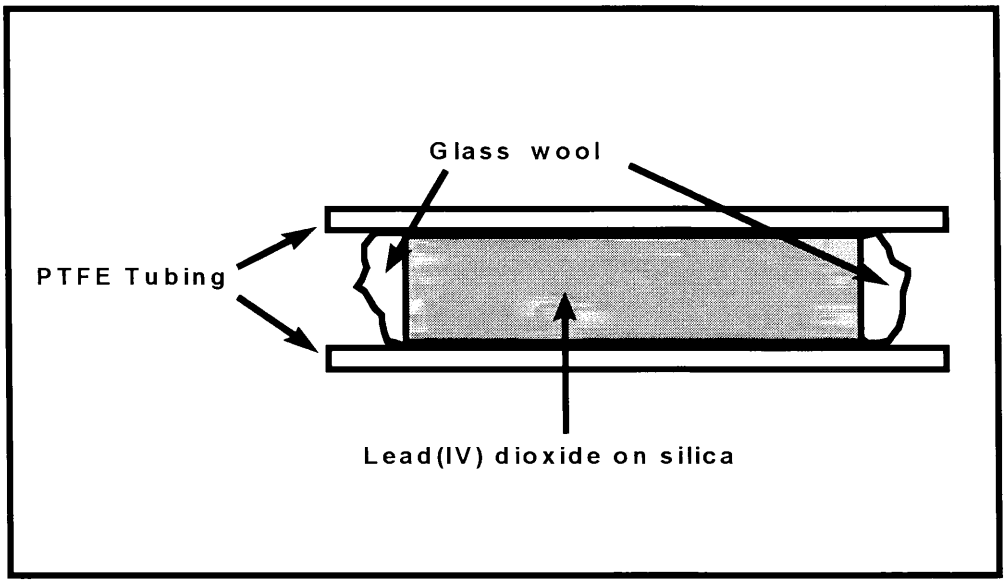

Figure 3.2: Construction of the solid-phase reactor

The solid-phase reactor (Fig 3.2) was constructed using PTFE (Teflon) tubing of internal diameter 1.52 mm. The reactor packing consisted of PbO_2 suspended on silicagel (mesh 30 - 70 ASTM; 0.2 - 0.5 mm, Merck, Darmstadt, Germany).

The preparation of this packing was done as described by Rüter and Neidhart [9], the only difference being that the NaOCl used in this work was purchased as a commercial

bleach. The bleach was added dropwise to a solution of 150 g lead(II)acetate in 500 mℓ water in which 75 g of the previously mentioned silicagel was suspended with fast stirring. The bleach was added until precipitation of the lead-(IV)dioxide had finished. The mixture was then stirred for a further 60 minutes, vacuumfiltrated, washed successively with dilute nitric acid and deionised water and the formed lead(IV)dioxide dried in a dessicator.

The packing of each reactor was done by attaching the Teflon tube to a vibrating shaker after plugging the bottom end with glass wool. The prepared packing was then introduced via a funnel. After packing each reactor had to be conditioned ('run in') before use for at least 45 minutes before use. This involved pumping deionised water through the reactor at a flow speed of 2.90 $m\ell\,min^{-1}$ for 30 minutes to ensure that there were no air pockets and to ensure a close packing of the glass beads. Following this was the pumping of carrier stream (HNO_3) through the reactor for 10 to 15 minutes.

The lifetime of each reactor could be established by comparing peak heights for the same standards from day to day. When the peak heights started to decrease systematically and drastically, the reactor had to be replaced. Another indication that the reactor was losing its oxidation capacity was the colour of the packing itself. At the start of the reactors' use the colour of the packing was dark brown (which looked purple through the Teflon tube). After a few days of use the colour of the packing at the front end of the reactor had disappeared, which meant that all of the PbO_2 had been stripped off the glass beads. When a third of the reactor was colourless it usually had

to be replaced. The total number of samples that could be processed with one reactor varied between 500 and 700, depending on the manganese concentration.

3.3 Optimisation

3.3.1 SPR parameters

The solid-phase reactor (SPR) forms the heart of the manifold of the proposed system and performance of the flow system depends on the efficiency of the redox reaction at the solid-liquid interface of the SPR. In addition to reactor packing, the reactor length, diameter and temperature were also major role players and had to be optimised.

3.3.1.1 Reactor length

The response and precision of the system were studied while varying the reactor length between 8 and 16 cm with the internal diameter fixed at 1.5 mm. A 5 $mg\ell^{-1}$ manganese(II) standard was used to optimise the system and the results obtained are shown in Table 3.1.

Two factors had opposing influences on the peak height, with longer reactors producing a longer reaction time of the manganese with the solid reagent that would lead one to expect a higher response. Longer reactors however, caused increased axial diffusion of the sample plug resulting in lower response. A compromise had to be

reached between these two factors, and an intermediate reactor length of 12 cm was chosen as the optimum, mainly because the best precision was achieved with this length.

Table 3.1: Optimisation of reactor length

Reactor length (cm)	Mean peak height	% RSD
8	0.6832	1.7
10	0.7661	2.2
12	0.7457	1.5
14	0.6865	1.7
16	0.7362	2.1

Figure 3.3 shows the response and precision for this optimisation.

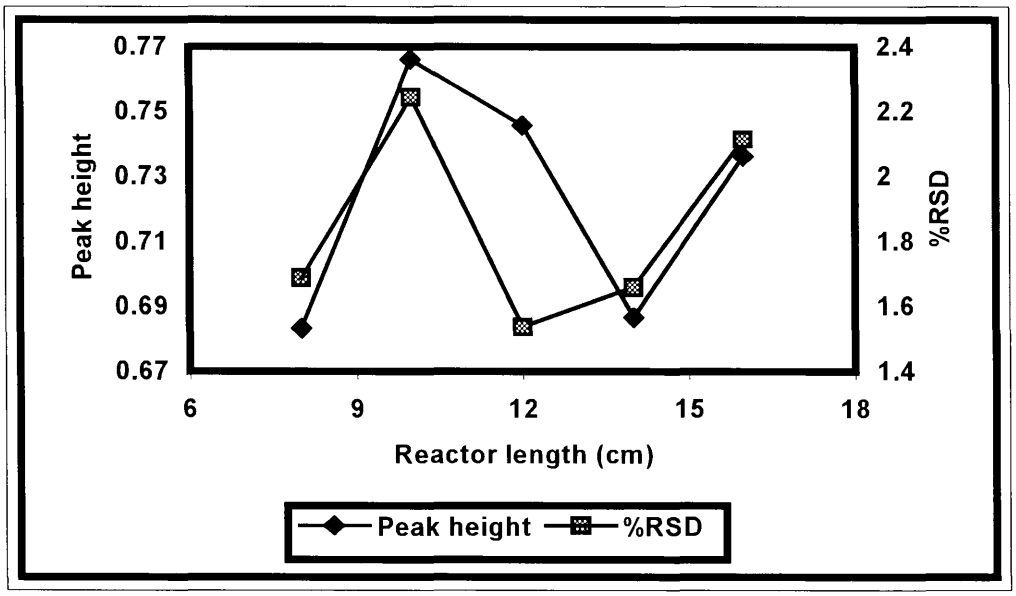

Figure 3.3: Optimisation data for reactor length

3.3.1.2 Reactor internal diameter

Preliminary experiments on reactors with an internal diameter of less than 1.3 mm indicated that solid-phase reactors with these dimensions were not suitable to incorporate into the conduits of the FIA system. The precision deteriorated dramatically, back pressure made the system useless for routine analysis and suitable reactor packing with 0.2 - 0.5 mm particles became difficult. The influence of smaller particles was also studied, but back pressure destabilised the system and the results obtained were poor.

The internal diameter of the reactor was then evaluated between 1.3 and 3.7 mm. The results obtained are given in Table 3.2. As is evident, the best response was obtained with the reactor of smallest diameter, while the best precision was obtained with reactors of an inner diameter between 1.5 and 1.9 mm. The response dropped with larger diameters due to increased dispersion. For further studies the reactor with an inside diameter of 1.9 mm was chosen because of the good precision obtained. Figure 3.4 shows the response and precision for this optimisation.

Table 3.2: Optimisation of the reactor internal diameter

Internal diameter (mm)	Peak height	% RSD
1.3	0.8637	2.0
1.5	0.8246	1.4
1.9	0.8232	1.4
2.3	0.7454	1.7
2.8	0.6684	1.6
3.7	0.5235	2.9

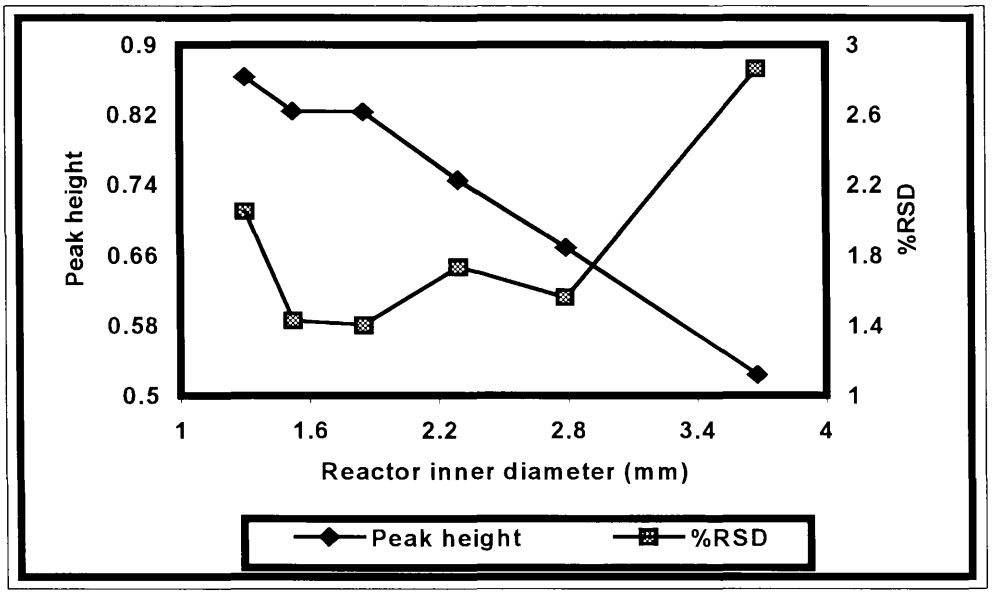

Figure 3.4: Optimisation data for internal diameter of reactor

3.3.1.3 Reactor temperature

The reactor temperature was varied between 50 and 75 °C, with the optimum results being obtained at 60 °C. The response increased with increasing temperature due to a faster reaction rate, but the precision showed a substantial decrease. Table 3.3 shows the results obtained with this study.

Table 3.3: Optimisation of reactor temperature

Temperature (°C)	Peak height	% RSD
50	0.5435	2.9
55	0.6209	1.8
60	0.6749	2.0
65	0.7657	2.7
70	0.8175	2.2
75	0.8555	3.2

In earlier work done by Rüter and Neidhart [1] the highest possible temperature of 90°C was used, but this temperature proved unacceptable for this work due to the poor precision and problems experienced with gas bubbles. The response and precision are depicted in Figure 3.5 to show the optimum value.

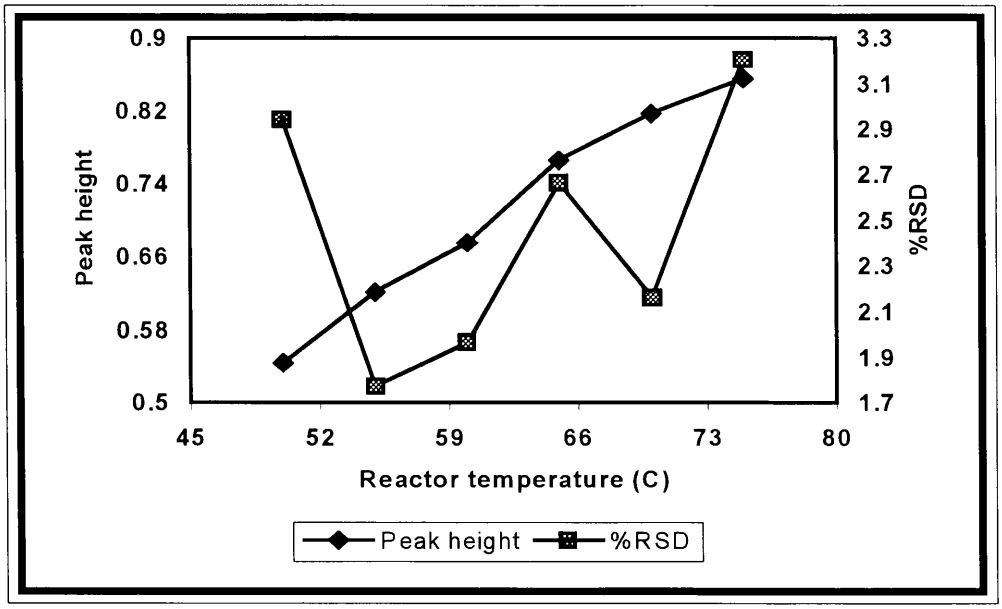

Figure 3.5: Optimisation of reactor temperature

3.3.2 Chemical parameters

3.3.2.1 Acid concentration of carrier stream

As mentioned in the introduction, acidic conditions are required for the oxidation of Mn^{2+}-ions to MnO_4^-. Care should be taken though, to ensure that the concentration of acid in the carrier stream is sufficient to give optimum performance without damaging the reactor. Originally a problem was experienced with bubble formation when the

carrier stream entered the heated reactor. This was attributed to a gas forming during the redox reaction in the reactor, but later it was established the bubble formation was due to dissolved gases in the carrier stream. The problem was circumvented by boiling the carrier solution before use to drive off all the dissolved oxygen.

Carrier solutions with HNO_3-concentrations between 0.05 and 0.5 mol ℓ^{-1} were evaluated. Results are given in Table 3.4.

Table 3.4: Optimisation of carrier concentration

HNO_3-concentration (mol ℓ^{-1})	Peak height	% RSD
0.05	0.5402	2.5
0.1	0.7189	0.92
0.2	0.7353	0.97
0.3	0.9212	1.2
0.4	1.023	1.4
0.5	1.042	1.8

Peak heights increased with increasing acid concentration, as was expected because of the pH-dependent nature of the reaction. The relative standard deviation for the carrier stream of 0.05 mol ℓ^{-1} was relatively poor at 2.5 %, which points to instability in the oxidation process. The precision improved dramatically to 0.92 % with an increase of HNO_3-concentration to 0.1 mol ℓ^{-1} in the carrier stream. There was an increase in response when the acid concentration was increased above 0.1 mol ℓ^{-1}, accompanied by a deterioration in precision, and these carrier streams were not considered for

further studies because of this relatively poor precision achieved. Figure 3.6 shows the response and precision achieved.

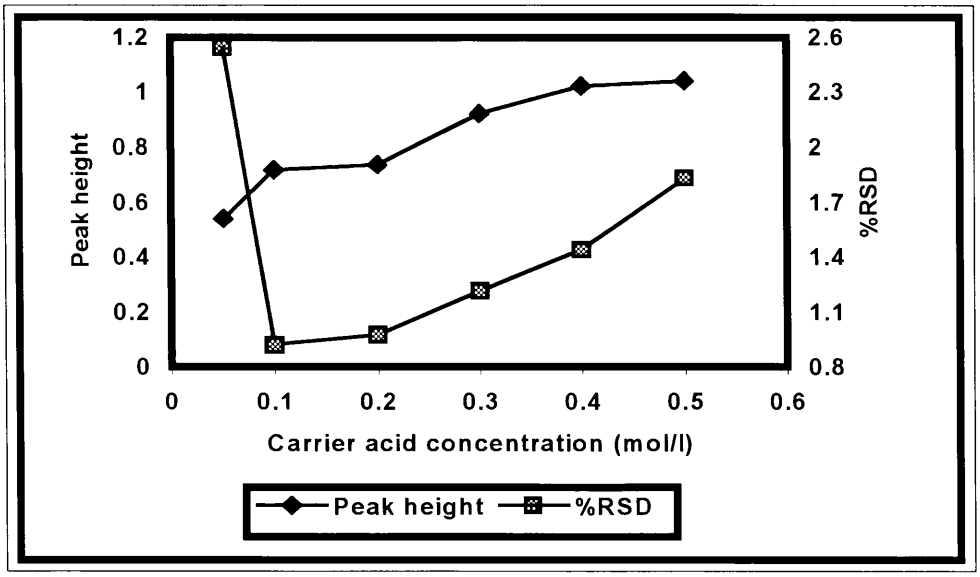

Figure 3.6: Optimisation of acid concentration

3.3.3 Physical parameters

3.3.3.1 Flow rate

The contact time between the sample zone containing Mn^{2+}-ions and the SPR is very important for the reaction to proceed sufficiently. As this depends on the flow rate of the sample zone through the SPR, a study of the flow rate of the carrier stream was conducted. The results for the optimisation are given in Table 3.5 and the optimisation graph in Figure 3.7. This particular optimisation presented an interesting dilemma, in that the peak profile for higher flow speeds was almost Gaussian, with a small tailing effect due to slow rinsing of the flow cell and longitudinal diffusion. At lower flow speeds the resulting peaks were wider, because of increased longitudinal diffusion, but

the peak heights increased substantially. The reason for this is that at lower flow speeds the manganese(II) takes longer to flow through the SPR, producing a longer reaction time, resulting in a higher yield of permanganate ions.

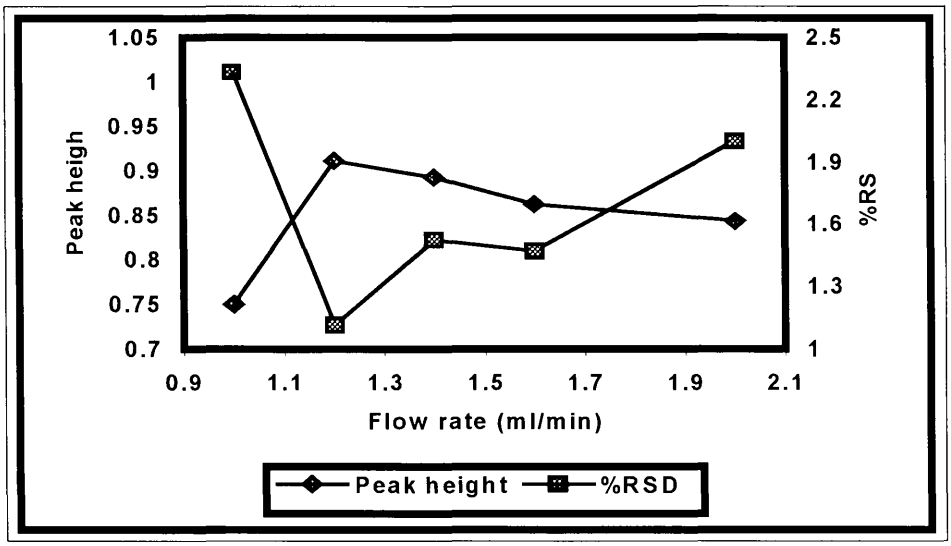

Figure 3.7: Optimisation of carrier flow rate

The optimum flow speed was found to be 1.20 $m\ell\ min^{-1}$, which is rather low, but this will ensure a low reagent consumption and is thus an advantage. The peak height at this flow speed was 0.91 and the relative standard deviation (RSD) was 1.2 %.

Table 3.5: Optimisation of flow rate

Flow rate ($m\ell\ min^{-1}$)	Mean peak height	% RSD
1.0	0.7500	2.3
1.2	0.9111	1.1
1.4	0.8929	1.5
1.6	0.8620	1.5
2.0	0.8427	2.0

3.3.3.2 Tube length

Optimisation of the tube length was done by distinguishing between two sections of tubing, namely the section from the injection valve to the SPR and the section from the SPR to the detector. A tube internal diameter of 0.76 mm was used for the length optimisation.

The tube length was varied between 22 and 40 cm with the shortest length giving the best results. This was expected as an increase in path length results in an increase in sample dispersion, producing a lower response. Shorter tubes were not used as the system configuration imposed a lower limit on the length. The results are given in Table 3.6 and in Figure 3.8.

Table 3.6: Optimisation of tube length (valve-SPR)

Tube length (cm)	Peak height	% RSD
22	0.5759	1.5
25	0.5626	3.2
30	0.5536	3.2
35	0.5188	3.2
40	0.4684	3.2

The optimum length for the section of tubing between the reactor and the detector was 50 cm, which was also the lower limit imposed by the system configuration.

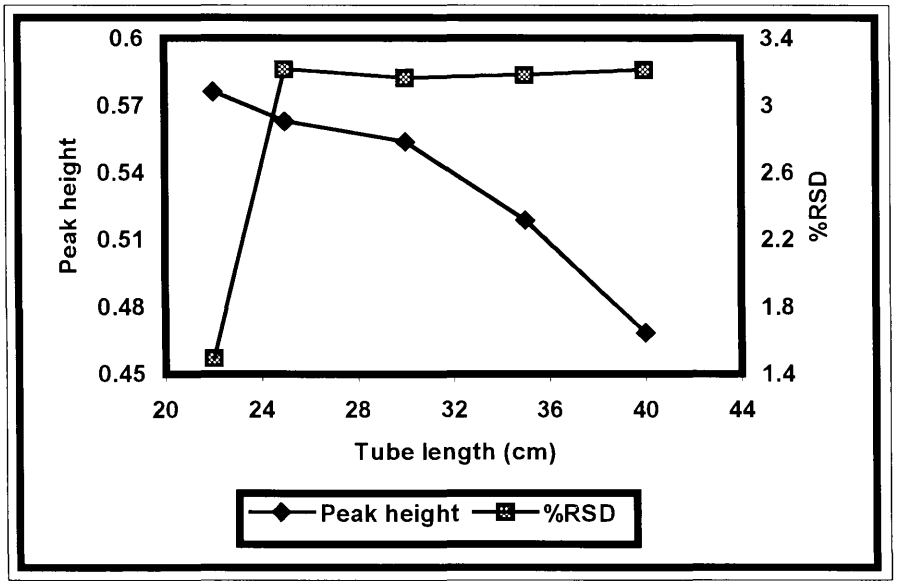

Figure 3.8: Optimisation of tube length (valve - SPR)

3.3.3.3 Tube internal diameter

The tube diameters for the two sections of tubing named above were evaluated using the optimum lengths determined. Tube diameters between 0.51 and 1.6 mm were evaluated for both sections.

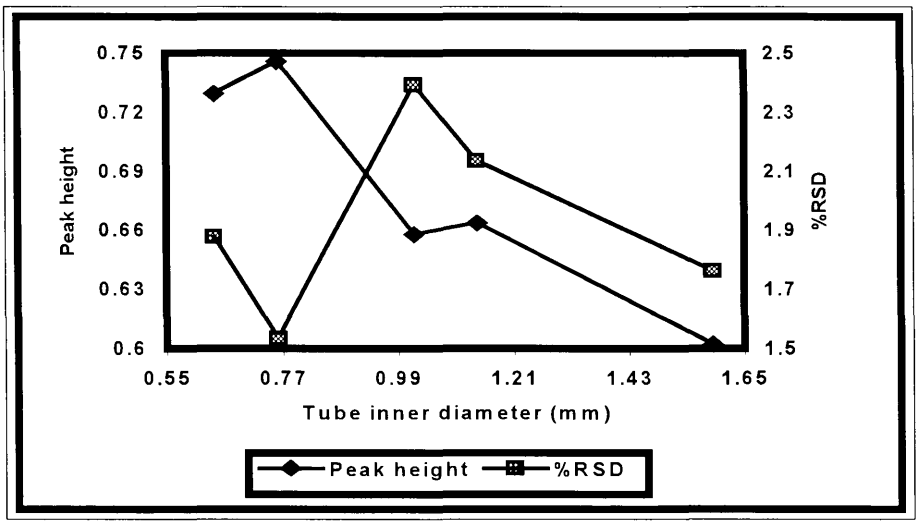

Figure 3.9: Optimisation of tube diameter (valve - SPR)

Optimum results for the section between the valve and the reactor were achieved with a diameter of 0.76 mm. The results are given in Figure 3.9 and Table 3.7.

Table 3.7: Optimisation of tube diameter (valve-SPR)

Tube diameter (mm)	Peak height	% RSD
0.64	0.7294	1.9
0.76	0.7457	1.5
1.0	0.6576	2.4
1.1	0.6636	2.1
1.6	0.6021	1.8

Optimum results for the section of tubing between the reactor and the detector were obtained with tubing of 0.76 mm inner diameter. Although the highest response was achieved with tubing of 0.51 mm the % RSD was higher than that achieved with tubing of 0.76 mm inner diameter and the latter value was taken as the optimum. The values for this optimisation are given in Table 3.8 and Figure 3.10.

Table 3.8: Optimisation of tube diameter (SPR-detector)

Tube diameter (mm)	Peak height	% RSD
0.51	0.7396	1.7
0.64	0.7266	1.6
0.76	0.7331	1.0
1.0	0.6066	3.0
1.1	0.5875	1.5

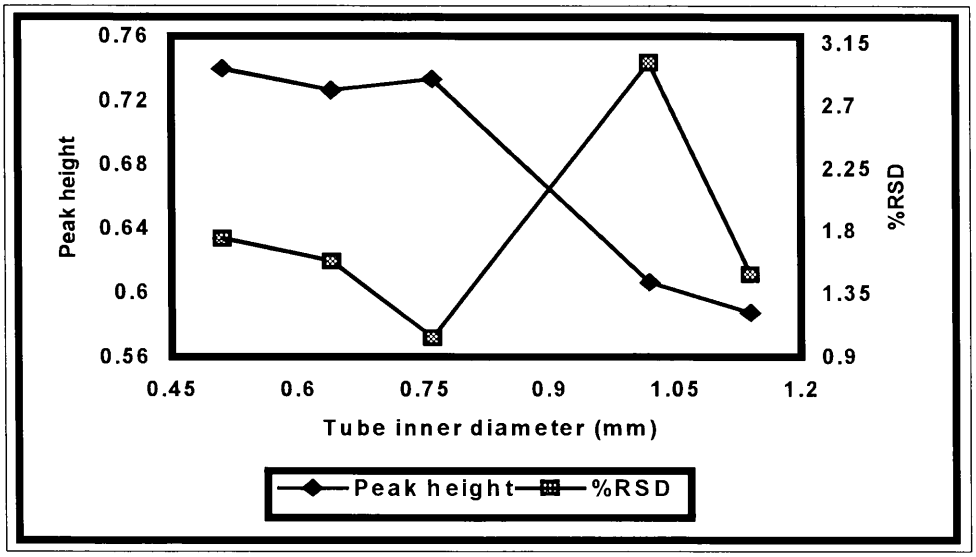

Figure 3.10: Optimisation of tube diameter (SPR-detector)

3.3.3.4 Sample volume

The values for this optimisation are given in Table 3.9 and Figure 3.11. The volume was varied between 55 and 95 $\mu\ell$. A value of 65 $\mu\ell$ was chosen as the optimum, because it gave by far the lowest % RSD.

Table 3.9: Optimisation of sample volume

Sample volume ($\mu\ell$)	Peak height	% RSD
55	0.5704	1.7
65	0.6699	0.93
75	0.7251	1.9
85	0.8291	1.6
95	0.8518	2.1

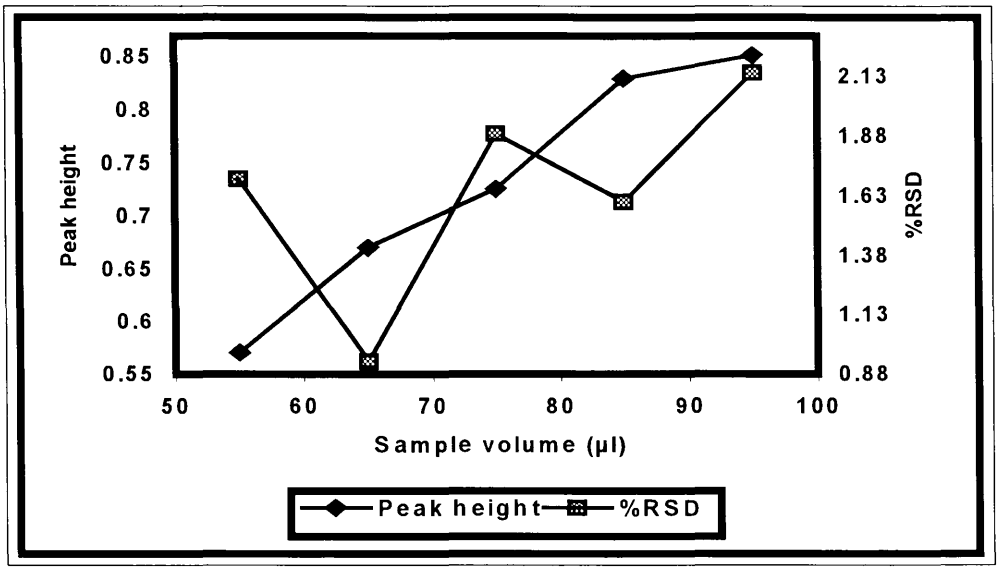

Figure 3.11: Optimisation of sample volume

3.4 Evaluation

The system was evaluated with regard to linear range, accuracy, precision, detection limit, sample interaction (carry-over), interferences, sampling rate and general problems experienced. The optimum conditions used are given in Table 3.10.

Table 3.10: Optimum conditions used for evaluation

Parameter	Optimum value
Reactor length	12 cm
Reactor diameter	1.52 mm
Acid concentration	0.1 mol ℓ^{-1}
Flow rate	1.20 mℓ min^{-1}
Sample volume	65 µℓ
Total tube length	72 cm
Tube diameter	0.76 mm

3.4.1 Linearity

The linearity of the FIA system was evaluated for analyte concentrations ranging from 1 to 100 mg ℓ^{-1} under optimum running conditions. The method was found to be linear in the range 1 to 5 mg ℓ^{-1}. The relationship obtained between response and concentration was:

$$y = 0.0965x + 0.0153 \qquad (3.1)$$

where y = peak height and x = analyte concentration (mg ℓ^{-1}). The correlation coefficient (r^2 = 0.993) indicated that the method was linear in this range. The calibration curve is shown in Figure 3.12.

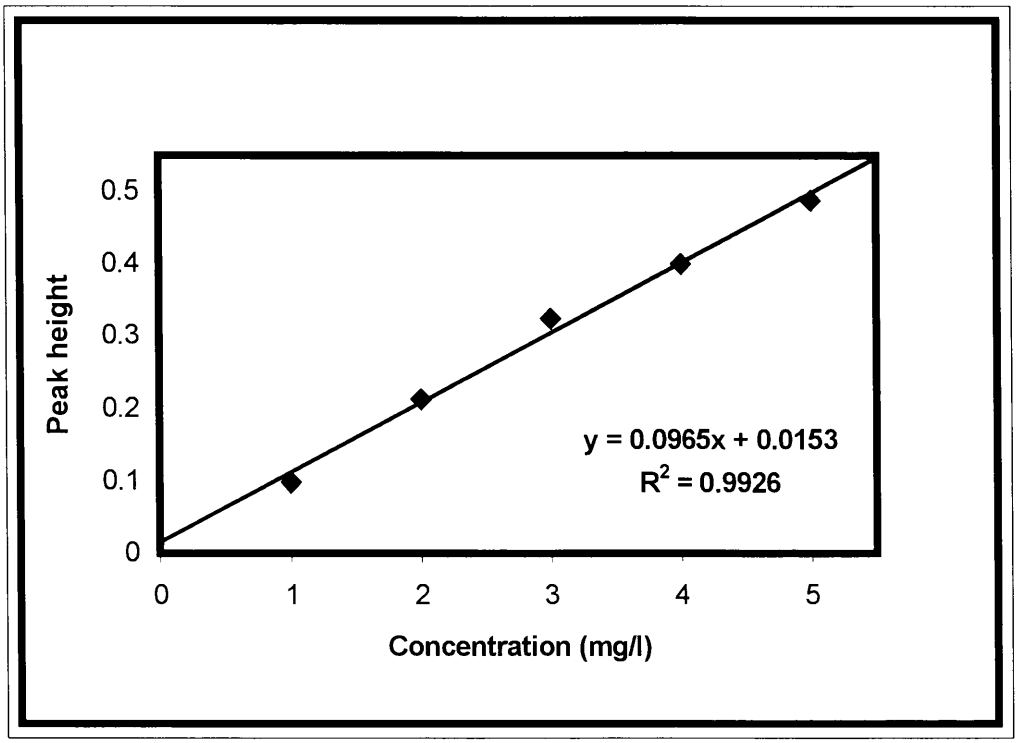

Figure 3.12: Calibration curve for manganese(II)

3.4.2 Accuracy

Real samples (samples from surface water and effluent streams) were analysed with the proposed system. The accuracy of the system was evaluated by comparing results obtained with the FIA system on real samples with the values obtained with a standard procedure. As can be seen in Table 3.10 and Table 3.11, the results compared favourably for normal surface samples and reasonably well for effluent streams.

Table 3.10: Comparison of results obtained with FIA method and a standard procedure for normal surface water.

Concentration of Mn in mg ℓ^{-1} (Standard procedure)	Concentration of Mn in mg ℓ^{-1} (FIA method)	%RSD for FIA method
4.6	4.2	1.56
1.3	1.1	1.75
3.7	3.7	1.59
1.8	1.9	1.71
3.2	2.9	1.65

Table 3.11: Comparison of results obtained with the FIA method and a standard procedure for effluent streams.

Concentration of Mn in mg ℓ^{-1} (Standard procedure)	Concentration of Mn in mg ℓ^{-1} (FIA method)	%RSD for the FIA method
37.44	37.40	1.69
66.68	53.05	1.73
131.7	115.6	1.72

The accuracy of the method was also determined by spiking one of the real samples and using the method of standard addition. A linear calibration curve was obtained

(correlation coefficient r = 0.998) and the concentration in the sample was determined as 1.1 mg ℓ^{-1} which compared well with both the FIA and standard procedures.

3.4.4 Recovery

The recovery on the system was also determined. Real samples were spiked with standard Mn^{2+} solutions, analysed and the recovery determined from the expected concentration. The formula used was:

$$\text{Recovery} = \frac{\text{experimental value}}{\text{expected value}} \times 100 \qquad (3.2)$$

The expected concentration of manganese(II) (4.5 mg ℓ^{-1}) for a tap water sample spiked with a small volume of a 1000 mg ℓ^{-1} Mn^{2+} standard was calculated with the calibration curve. The sample was then analysed and the concentration (4.31 mg ℓ^{-1}) was compared with the expected concentration as shown above. The recovery ranged between 95.7 and 103% which was acceptable.

3.4.5 Precision

The precision of the method was determined by doing 11 repetitions of standard solutions as well as 11 repetitions of samples under optimum conditions. The average peak height for the 5 mg ℓ^{-1} standard was 0.505 and the standard deviation was 0.009.

The precision was then obtained by calculating the % RSD with the following equation

$$\% \text{ RSD} = \frac{\text{Peak height}}{\text{Standard deviation}} \times 100 \qquad (3.3)$$

This gave a value of 1.78 for the %RSD on the standard solution. The average peak height obtained for the sample was 0.513 and the standard deviation 0.009. This gave a value of 1.75 for the % RSD as calculated with the equation above.

3.4.6 Sample interaction

The sample interaction or carry-over was calculated according to the following formula:

$$\text{Interaction} = \frac{A_3 - A_1}{A_2} \times 100 \qquad (3.4)$$

where A_1 = peak height for sample without interaction

A_2 = peak height for a sample with ten times the concentration of A_1

A_3 = peak height for interacted sample with the same concentration as A_1

In this study A_1 and A_3 was obtained with a 10 mg ℓ^{-1} manganese(II) standard and A_2 was obtained with a 100 mg ℓ^{-1} manganese(II) standard. The values for A_1 and A_3 were 0.815 and 0.880 respectively. The value for A_2 was 6.85, giving an interaction value of 0.95 % at a sampling rate of 30 samples per hour, which is negligible.

3.4.7 Detection limit

The detection limit of a method is defined as the lowest concentration of analyte that can be determined with a certain risk of error. This was determined for the method under discussion using the formula:

$$\text{Detection limit} = \frac{(3\sigma + K)(K - c)}{m} \qquad (3.5)$$

where σ (1.2 %) is the relative standard deviation of the baseline, K (0.03) is the average signal value of the baseline and *c* (0.0153) and *m* (0.0965) are the intercept and slope of the calibration curve respectively. The detection limit was calculated as 0.55 mg ℓ^{-1}.

3.4.8 Interferences

According to work done by Rüter and Neidhart [9] the only interferences for the determination of permanganate at 520 nm are reducing substances and coloured metal ions (Fe^{3+}, Ni^{2+} ,V^{5+} ,Cu^{2+} ,Co^{2+}) in high concentrations as well as anions (halogens, SO_4^{2-}, PO_4^{3-}, CO_3^{2-}, CH_3COO^-, SCN^-, $C_2O_4^{2-}$, SO_3^{2-}). The reducing substances would conceivably interfere by reducing some of the formed MnO_4^- and thereby lowering the absorbance. The coloured metal ions would raise the absorbance if they were present in the sample and thus interfere positively. The interfering effects of these ions on real samples were investigated, but only a few of the ions had any influence in the samples analysed.

The only two ions that may pose a threat are when Fe^{2+} and Fe^{3+}-ion concentrations in mining drainage samples rise above 250 mg ℓ^{-1} for Mn^{2+} ion values of below 5 mg ℓ^{-1}, or when V^{5+}-ions are present in concentrations above 25 mg ℓ^{-1}. Thus for the determination of manganese in water samples there should be no interferences after appropriate dilution.

3.4.9 Sampling rate

The time taken for each run varied between 100 seconds for samples with low Mn^{2+} concentrations and 150 seconds for samples with higher concentrations. The increased times are due to longer return-to-baseline times, implying longer washing-out times for the flowcell. Thus, a range of sampling rates are obtained, varying between 24 and 36 samples per hour, depending on the Mn^{2+} concentration.

3.4.10 General problems

As was previously mentioned, the biggest problem encountered with this system was the bubbles that formed when the carrier passed through the waterbath. As was also mentioned, the problem could be overcome by boiling the HNO_3 prior to use. Another problem was encountered after leaving a SPR in a laboratory for a particularly cold weekend. The SPR was used in the flow system, but no response was shown, even for very high Mn^{2+} concentrations. All the components of the system were checked, and it was established that the problem could only lie at the SPR. The PbO_2 used for the

packing of the reactor was tested by hand under normal operating conditions and it was seen that the reaction time had increased substantially. Thus, what had happened in the system was that the sample had passed through the SPR before the redox reaction could take place. A new batch of reactor packing was prepared, and stored in a temperature-controlled laboratory from then on. This batch worked well for further analysis.

3.5 Conclusion

As can be seen from the above discussion the method can be used for the determination of manganese(II) in aqueous samples that are free from particulate matter. The sampling rate is a bit low, but the big advantage of this system is its relative simplicity and ease of use. Another drawback of the system is its low dynamic range, which means that almost all samples have to be diluted prior to analysis, with the possibility of errors arising. It is believed that the advantages of the system (simplicity, ease of use, relative low cost of reagents etc.) outweigh the negative points.

3.6 References

[1] E. Griffen, **J. Am. Water Work Assoc., 52** (1960) 1326.

[2] A. R. Bowie, P. R. Fielden, R. D. Lowe and R. D. Snook, **Analyst, 120** (1995) 2119.

[3] A. Gaikwad, M. Silva and D. Perez-bendito, **Anal Chim. Acta, 302** (1995) 275.

[4] J. Ruzicka and E. H. Hansen, **Flow-injection analysis,** 2nd Ed, Wiley, New York, 1988.

[5] M. Valcárcel and M. D. Luque de Castro, **Flow Injection Analysis. Principles and applications,** Horwood, Chichester, 1987.

[6] J. L. Burguera, **Flow-Injection Atomic Spectrometry,** Marcel Dekker, New York, 1989.

[7] M. D. Luque de Castro, **Trends in Analytical Chemistry, 11** (1992) 149.

[8] J. Martínez Calatayud and J. V. García Mateo, **Trends in Analytical Chemistry, 12** (1993) 428.

[9] J. Rüter and B. Neidhart, **Microchimica Acta, 18** (1984) 271.

[10] J. Rüter, U. P. Fislage and B. Neidhart, **Microchimica Acta,** (1984) 389.

[11] G. D. Marshall and J. F. van Staden, **Analytical Instrumentation, 20** (1992) 79.

CHAPTER 4

The determination of sulphide in effluent streams using a solid-phase lead(II)chromate reactor incorporated into a flow system.

4.1 Introduction

The sulphide ion is found in natural waters due to anaerobic decomposition of sulphur-containing compounds, where it may cause, among others, browning disease in rice [1]. It can also contribute towards corrosion due to deformation of acids and alkalis [1]. Sulphide is also found in industrial effluents due to the processing of petroleum [2] as well as the Kraft process as used in paper and pulp industries [3]. Because of the bad odour and extreme toxicity due to complexation with metal ions vital to human metabolism [1], the determination of sulphide and H_2S down to trace level is important.

A number of standard methods are available for this, such as voltammetry [4], spectrophotometry [2,3,5-7], HPLC [8], titrimetric determination [9], optical fibre sensoring [10] and ion-selective electrodes [11]. Because of the ease of use and possible

automation with flow systems most of these methods have been adapted for use with such systems [1,4,5-8].

The use of solid-phase reactors incorporated into flow injection manifolds [13,14] may offer certain advantages over homogeneous systems where the sample and the reagent are both in the liquid phase. Reagent consumption is greatly reduced and the system is simplified with fewer junctions for mixing of reagent, sample and carrier streams.

This chapter reports on the use of a flow injection system for the determination of sulphide in dairy effluents. As with previous work [15], the reagent was immobilised in a reactor and only reacted when a sample passed through the reactor. The aim was to minimise reagent consumption as well as to simplify the flow system. The solid phase in this case was lead(II)chromate, immobilised on fused alumina. The sulphide determination was done indirectly, with the analyte ions releasing chromate ions into the carrier stream by forming insoluble PbS (K_{sp}(25 °C) = 7×10^{-28}) in the reactor. The released CrO_4^{2-}-ions were detected spectrophotometrically at 370 nm. The reaction equation is

$$PbCrO_4(s) + S^{2-}(aq) \Leftrightarrow PbS(s) + CrO_4^{2-}(aq)$$

The solubility product for $PbCrO_4$ (K_{sp}(25°C) = 1.8×10^{-14}) is higher than that for PbS mentioned above, and this was the driving force for the reaction.

A similar system was used for the determination of sulphate in surface- and seawater [13]. In that study the solid phase was $BaCrO_4$($K_{sp} = 2.4 \times 10^{-10}$) and the reaction with sulphate

produced $BaSO_4$(K_{sp} = 1.1 × 10^{-10}). The same solid phase could not be used for sulphide determination however, because barium sulphide does not form a precipitate.

4.2 Experimental

4.2.1 Reagents and solutions

All reagents were prepared from analytical-reagent grade chemicals unless specified otherwise. Deionised water from a Modulab system (Continental Water Systems, San Antonio, TX, USA) was used to prepare all solutions and dilutions.

4.2.1.1 Preparation of the sulphide stock solution

A stock solution containing 1000 mg ℓ^{-1} of sulphide was prepared by taking a quantity of partially hydrated sodium sulphide scales, wetting it with deionised water for full hydration and then weighing 7.490 g of these in a glass beaker. The scales were then dissolved in deoxygenated water and diluted to 1 ℓ. The deoxygenated water was prepared by bubbling nitrogen gas through doubly deionised water for 30 minutes to remove all of the dissolved oxygen that could cause oxidation of the sulphide.

The prepared sulphide solution was standardised with the aid of an iodometric titration technique, using starch as indicator. The concentration of the stock solution was

1000 mg ℓ^{-1} and this solution was kept under an inert atmosphere to prevent oxidation. Working sulphide solutions in the range 10 - 50 mg ℓ^{-1} were prepared by diluting appropriate amounts of the stock solution with deionised water. These working solutions were prepared daily, because the sulphide concentration in these solutions decreased rapidly due to the oxidation of sulphide to sulphite and sulphate.

4.2.1.2 Carrier stream composition

The carrier stream used had the same composition as that used by Sakuragawa *et al* [16] for the determination of sulphate in seawater. It was prepared by weighing 0.738 g of sodium acetate (BDH Chemicals, Poole, England), adding 80 mℓ of ethanol and diluting to 2 dm^3 with deionised water. This gave a solution of 4.5 mmol ℓ^{-1} $NaCH_3COO$ in 4% ethanol.

4.2.1.3 $PbCrO_4$ solid phase

The solid phase reagent was immobilised on fused alumina. 1.202 g potassium chromate (Saarchem, South Africa) was weighed in a beaker and dissolved in 100 mℓ deionised water. In another beaker 2.050 g lead nitrate (B. Owen Jones, South Africa) was weighed and 5 g alumina was added together with 100 mℓ deionised water. This mixture was stirred on a magnetic stirrer, with heating, while the K_2CrO_4 solution was added dropwise over a period of 30 minutes.

The produced $PbCrO_4$ precipitated onto the alumina beads and this was filtered and dried overnight.

4.2.2 Instrumentation

The FIA system was constructed from the following components: a Cenco peristaltic pump operating at 10 rpm, a VICI 10-port 2-position sampling valve, a Unicam 8625 UV-visible spectrophotometer equipped with 10 mm Hellma type flow-through cell (volume 80 µl) for absorbance measurements and a FlowTEK [17] software package.

4.2.3 Operation of the system

A schematic diagram of the flow-injection system is given in Fig. 4.1. The configuration of the system closely resembles that of the system described in chapter 3, the only difference being the omission of the waterbath.

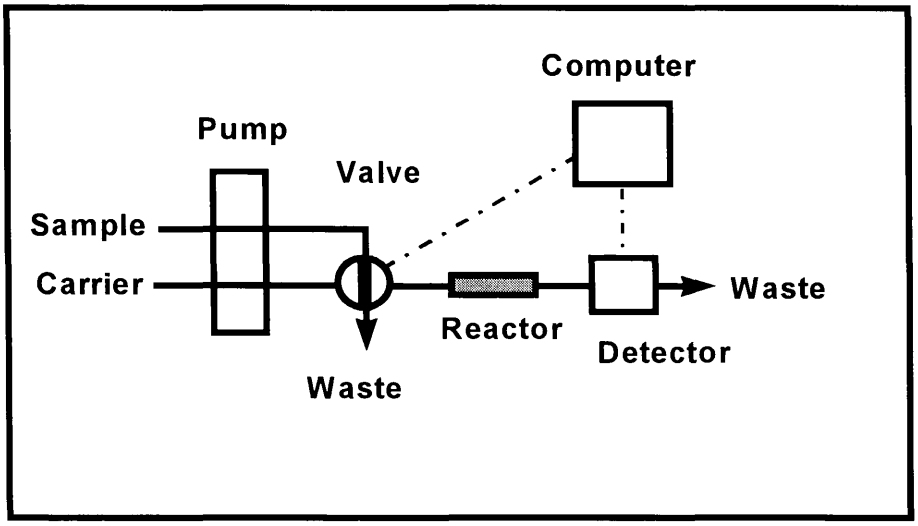

Figure 4.1: Diagram of the FIA system

The sample- and carrier streams were pumped through the manifold at 0.60 and 0.80 $m\ell\ min^{-1}$ respectively. The total time for each sampling run was 115 seconds of which the first 5 seconds were for stabilising the baseline, the next 45 seconds for injecting the sample plug and the last 65 seconds for flushing the system and loading the sample. The injected sample plug was pumped through the solid-phase reactor, packed with $PbCrO_4$ on alumina, where the sulphide reacted with the lead to form insoluble lead sulphide. The chromate was released into the carrier stream and the increase in absorbance was measured at 370 nm. The data obtained was converted to a relative response (arbitrary units) vs. time graph with the aid of the FlowTEK software package and the maximum peak height was stored on computer.

4.2.4 The solid phase reactor

This reactor was constructed using Tygon manifold tubing (Technicon) with an inner diameter of 2.1 mm and a length of 60 mm. The packing consisted of the previously mentioned lead chromate suspended on alumina. The packing of the reactor was done by placing a ball of glass wool in one end of the tube, attaching the other end to a funnel which in turn was connected to a vibrating shaker, and introducing the suspended lead chromate through the funnel while shaking. The top end of the reactor was then plugged with glass wool as well. Before use for measurements the reactor had to be conditioned by doing 50 repetitive injections of a 30 $mg\ell^{-1}$ S^{2-} solution. After this 'running-in' or conditioning period the reactor showed repeatable behaviour for 150-200 runs, depending on the sulphide concentration. The day-to-day reproducibility of the reactor was acceptable as long as the total number of samples analysed with the reactor did not exceed 200.

4.3 Optimisation

4.3.1 Solid-phase reactor (SPR) parameters

As was the case with previous work [10,15] done on solid phase chemistry in flow systems, the SPR forms the heart of the system and thus the greatest amount of time was spent optimising the parameters related to it.

4.3.1.1 Reactor length

The sensitivity and precision of the method were firstly studied by keeping the reactor inner diameter fixed at 2.54 mm and varying the length between 50 mm and 120 mm. The results can be seen in Table 4.1 and Figure 4.2.

Table 4.1: Optimisation of reactor length

Reactor length (mm)	Peak height	% RSD
50	0.3348	2.8
60	0.3396	2.0
70	0.2260	1.7
80	0.1617	4.0
90	0.1507	4.9
100	0.2348	2.6
110	0.1436	1.7

A 120 mm reactor gave problems due to back-pressure and thus longer reactors were not used. The best responses were obtained with the 50 mm and 60 mm reactors (0.3348 and 0.3396 respectively), while the best precision was obtained with the 70 mm and 110 mm reactors. The 60 mm reactor was chosen as the optimum because of the high response and relatively good precision.

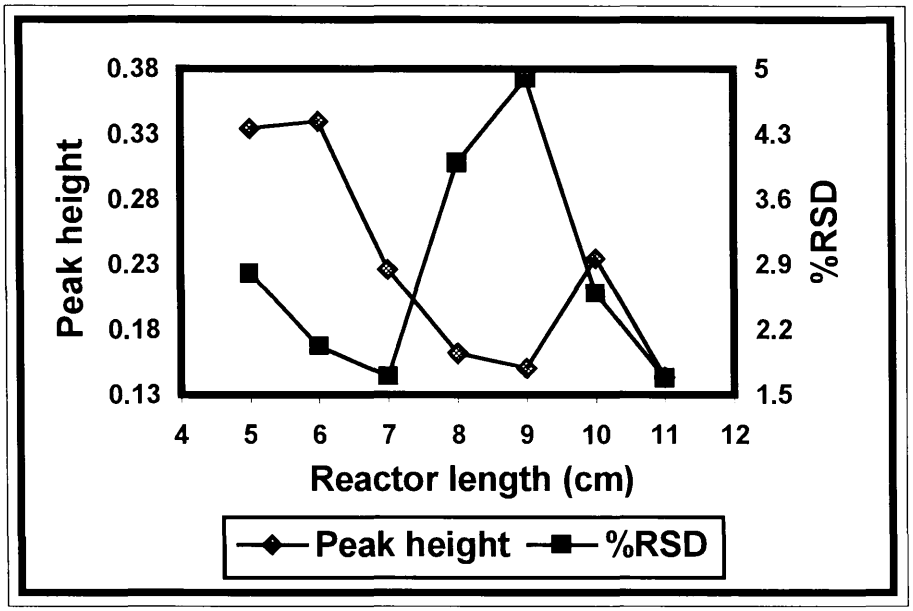

Figure 4.2: Optimisation of reactor length

4.3.1.2 Reactor internal diameter

The reactor inside diameter was then varied between 1.5 mm and 2.5 mm while keeping the length fixed at the optimum value obtained above. The results can be seen in Table 4.2 and Figure 4.3.

Table 4.2: Optimisation of reactor internal diameter

Diameter (mm)	Peak height	% RSD
1.7	0.08992	3.8
1.9	0.1380	5.3
2.1	0.2220	2.9
2.3	0.1578	4.4
2.5	0.1467	3.1

The reactor with an inner diameter of 1.5 mm caused leakage in the system between the valve and reactor due to back-pressure. Reactors with smaller inside diameters were thus not used. The optimum results were achieved with a reactor of intermediate diameter (2.1 mm). The relative response was the highest (0.2220) and the precision the best (% RSD: 2.9).

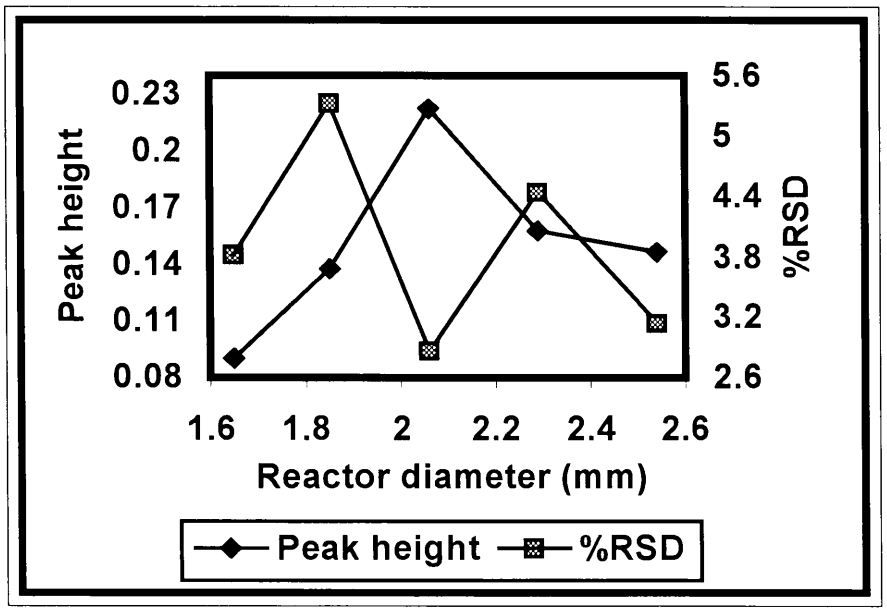

Figure 4.3: Optimisation of reactor inner diameter

4.3.2 Chemical parameters

4.3.2.1 Carrier stream composition

Experiments indicated that the optimum reagent concentration for the carrier stream solution was a 4.5 mmol ℓ^{-1} $NaCH_3COO$ solution in 4% volume per volume ethanol

which confirmed the results obtained by Sakuragawa *et al* [16] for the determination of sulphate. The pH of the solution was 8.2, which was not basic enough to damage the SPR by forming $Pb(OH)_2$ and also not acidic enough to react with the sulphide in the sample to form H_2S.

4.3.3 Physical parameters

4.3.3.1 Flow rate

As mentioned in the previous chapter the contact time between the sample plug and the solid-phase reactor is of the utmost importance for the reaction to the optimum analytical results. This period was influenced by the SPR parameters already discussed as well as the flow rate. The flow rate was varied between 0.8 $m\ell\ min^{-1}$ and 2.0 $m\ell\ min^{-1}$ and the results are given in Table 4.3 and Figure 4.4.

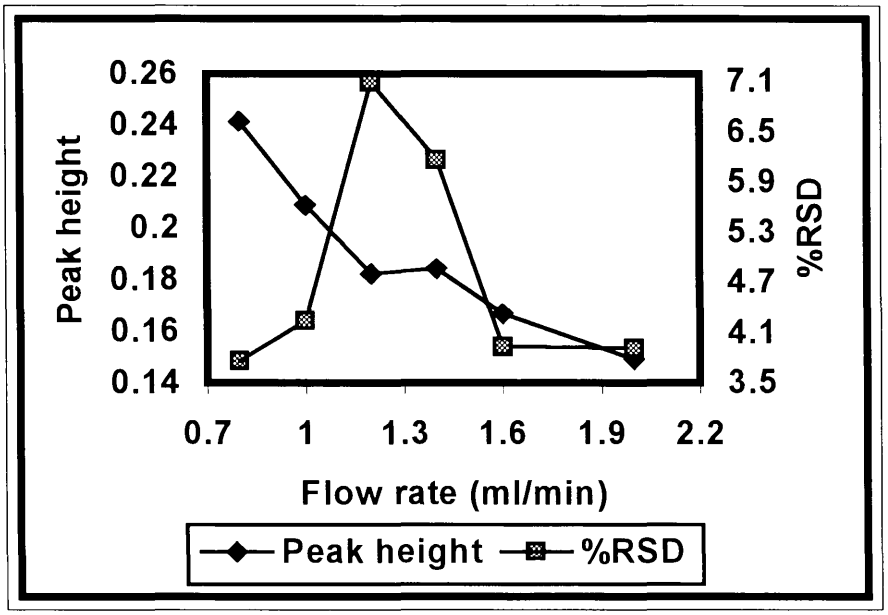

Figure 4.4: Optimisation of flow rate

The lower flow rates produced the highest peaks because of the relatively long contact time with the reactor, with 0.8 $m\ell\ min^{-1}$ being the optimum rate. The relative peak height obtained was 0.2414 and the % RSD was 3.8.

Table 4.3: Optimisation of flow rate

Flow rate ($m\ell\ min^{-1}$)	Peak height	% RSD
0.80	0.2414	3.8
1.0	0.2088	4.2
1.2	0.1821	7.1
1.4	0.1841	6.2
1.6	0.1666	4.0
2.0	0.1489	4.0

4.3.3.2 Tube length and diameter

The total length of the transmission tubing used was 40 cm which was the lower limit imposed by the configuration of the system. The internal diameter of the tubing was 0.76 mm.

4.3.3.3 Sample volume

The sample volume was varied between 65 and 105 $\mu\ell$, with the bigger volumes giving higher responses as expected, unfortunately coupled with lower precision. The results are given in Table 4.4 and Figure 4.5. The sample volume of 75 $\mu\ell$ was chosen as the optimum value, giving the best compromise between high response and good precision with a relative response of 0.2606 and a % RSD of 2.7.

Table 4.4: Optimisation of sample volume

Sample volume ($\mu\ell$)	Peak height	% RSD
65	0.2013	2.3
75	0.2606	2.7
85	0.2942	3.1
95	0.3019	5.4
105	0.3313	2.9

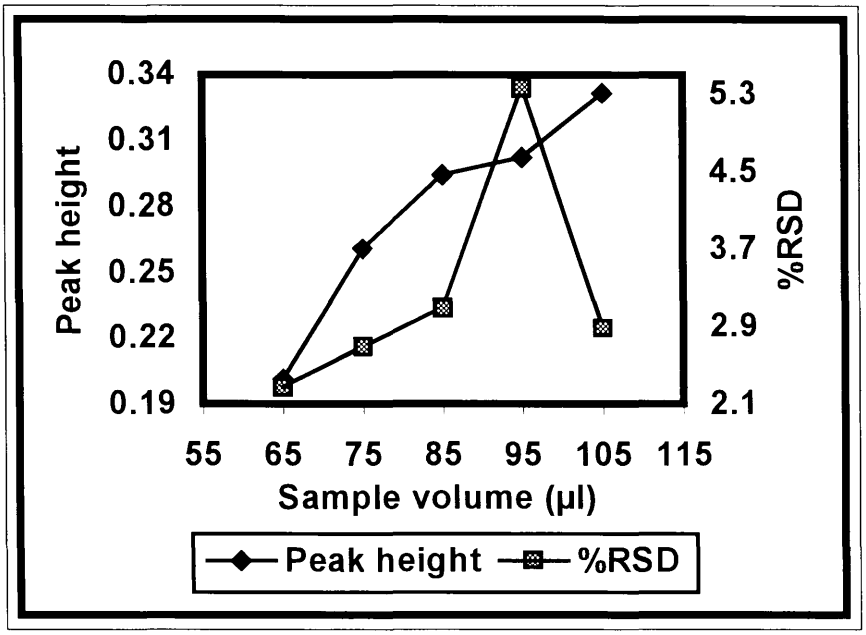

Figure 4.5: Optimisation of sample volume

4.4 Method evaluation

The method was thoroughly evaluated with regard to parameters such as accuracy, linearity, recovery, and interferences. The conditions used are given in Table 4.5.

Table 4.5: Optimum conditions used for method evaluation

Parameter	Optimum value
Reactor length	60 mm
Reactor inner diameter	2.06 mm
Carrier pH	8.2
Sample pH	8.4
Flow rate	0.8 mℓ min^{-1}
Tube length	40 cm
Tube diameter	0.76 mm
Sample volume	75 µℓ

4.4.1 Linearity

The linearity of the system was evaluated between 5 and 60 mg l^{-1} under optimum conditions. The method was found to be linear in the range 10 to 50 mg l^{-1}.

The relationship obtained between response and concentration was:

$$y = 0.007019 + 0.03198x \qquad (4.1)$$

where y = peak height and x = sulphide concentration in mg l^{-1}. The correlation coefficient (r^2 = 0.987) indicated that the method was linear in the range 10 to 50 mg ℓ^{-1}. The calibration curve is shown in Figure 5.5

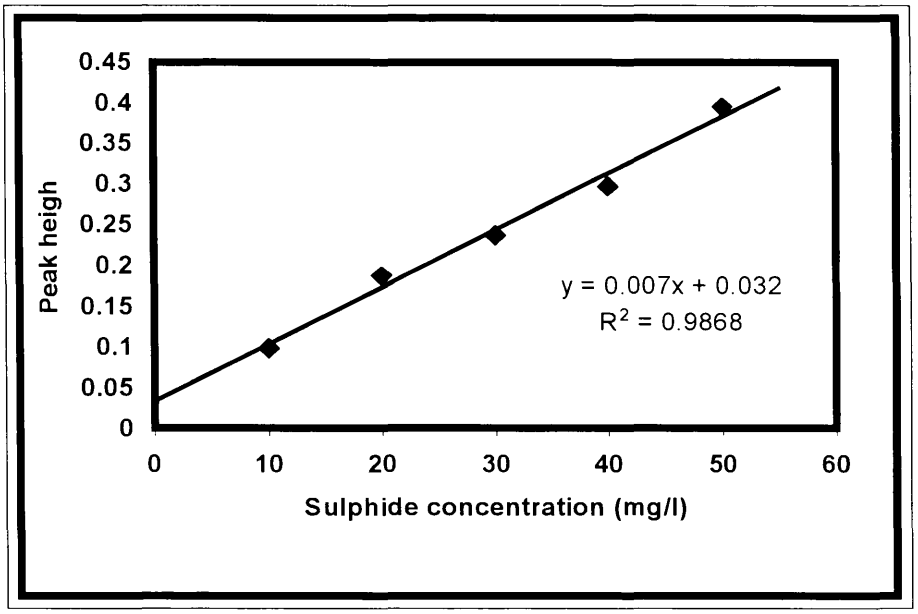

Figure 4.6: Calibration curve for sulphide

4.4.2 Accuracy

Real effluent samples from a dairy farm were analysed with the system and also with a standard manual method (iodometric titration). The results were then compared to determine the accuracy of the automated method. The results are given in Table 4.5 and compare reasonably well.

Table 4.5: Comparison of results obtained for effluent streams with the proposed system and a standard procedure

Standard method (manual) $[S^{2-}]$ as mg ℓ^{-1}	Flow-injection method $[S^{2-}]$ as mg ℓ^{-1}
22	19
15	14

The accuracy was also determined by spiking tap water samples with 1000 mg ℓ^{-1} sulphide and analysing. The percentage recovery varied between 83 and 96%.

4.4.3 Precision

The precision was determined by doing 12 repetitions of a 30 mg ℓ^{-1} sulphide standard under optimum running conditions, as well as 12 repetitions of a sample. The % RSD obtained for the standard was 2.9 %, and that obtained for the sample was 5.3 %. These values are high compared with previous solid-phase work [15], but the immobilising and packing of the solid phase could not be done as readily and easily as the author would have liked, and uneven packing and coating of the support material would contribute to poor precision.

The day-to-day reproducibility of each reactor was also evaluated, but as the number of samples that could be analysed with a single reactor was low, the reactor could not be used for more than two successive days. The reproducibility for the two days was good, considering the standards were freshly prepared each day and could have differed from day to day.

4.4.4 Sample interaction

The sample interaction (carry-over) was calculated with the following equation:

$$\text{Interaction} = \frac{A_3 - A_1}{A_2} \times 100 \qquad (4.2)$$

where A_1 = peak height obtained with a 10 mg ℓ^{-1} S^{2-} standard

A_2 = peak height obtained with a 100 mg ℓ^{-1} S^{2-} standard after obtaining A1

and A_3 = peak height obtained with a 10 mg ℓ^{-1} S^{2-} standard after obtaining A2.

In this case, A_1 was 0.0757, A_2 was 0.4077 and A_3 0.0903. This gave a value of 3.6 % for the sample interaction at a sampling rate of 30 samples per hour.

4.4.5 Detection limit

The detection limit was calculated using the formula:

$$\text{Detection limit} = \frac{(3\sigma + K)(K - c)}{m} \qquad (4.3)$$

with σ denoting the relative standard deviation of the baseline signal, K the average baseline signal and *c* and *m* denoting the intercept and slope of the calibration curve respectively. The value for the baseline signal was 0.022 units and the relative standard deviation was 2.6 %. The intercept and slope of the calibration curve were 7.02×10^{-3} and 3.20×10^{-2} respectively, as mentioned in the paragraph on linearity. These values, when substituted into equation 4.1, gave a detection limit of 3.66 mg ℓ^{-1}.

4.4.6 Interferences

A range of anions and cations were tested for interference in different concentrations. Standard sulphide solutions containing 30 mg ℓ^{-1} were spiked with different amounts of interferents to determine the admissible concentrations of these interferents. The data obtained is given in Tables 4.6 and 4.7. As is evident, the most serious anion interference is caused by the hydroxide ion in high concentrations. The interference is positive because of the formation of $Pb(OH)_2$ (K_{sp} (25 °C) = 2.8 x 10^{-16}) [13], which releases chromate more readily into the carrier stream than sulphide does.

Table 4.6: Anions tested for interference

Anion	Concentration (mg ℓ^{-1})	%Recovery of S^{2-}	Concentration (mg ℓ^{-1})	%Recovery of S^{2-}
S^{2-}	30	100	30	100
Cl^-	300	105	30	102
SO_4^{2-}	300	91.8	30	97.1
NO_3^-	300	94.1	30	87.5
OH^-	300	221	30	112
CO_3^{2-}	300	135	30	97.2
Br^-	300	110	30	93.0

This is the reason why the carrier stream- and sample pH can not be higher than 8.5. The carbonate ion gives a positive interference as well, for the same reason mentioned above, though the effect is not as pronounced.

The cations tested for interference were calcium, magnesium and iron(III). All three ions interfere seriously, with the iron forming a black precipitate at high concentrations, causing the iron/sulphide samples to be discarded. The precipitate is probably Fe_2S_3 (K_{sp} (25 °C) = 1.4 x 10^{-88})[13]. The calcium and magnesium probably interfere because of complexation with the released chromate. At lower concentrations however, the effect is not as serious, as can be seen in Table 4.7. The concentrations of these cation interferences in the samples analysed were not high enough to affect the performance of the system.

Table 4.7: Cations tested for interference

Ion	Concentration (mg ℓ^{-1})	%Recovery of S^{2-}	Concentration (mg ℓ^{-1})	%Recovery of S^{2-}
S^{2-}	30	100	30	100
Ca^{2+}	300	48	30	94.1
Mg^{2+}	300	56.5	30	81.8

Sakuragawa *et al* [16] circumvented the problem of cation interferences by using a cation exchange column in front of the reactor. This could not be done in this study as an evenly packed column would have caused too much back-pressure for the peristaltic pump and Teflon fittings to handle. An extra column in the manifold also enlarges the system, which is counterproductive to the aims set at the start, namely simplification and miniaturisation.

4.5 Conclusion

The method was reasonably accurate in determining sulphide in dairy effluent when compared to manual methods. There are a few problems associated with the system, such as the low number of samples that can be analysed with a single reactor, the long conditioning period and the relatively poor precision obtained. The method is not as sensitive as expected, mainly because of the indirect nature of the detection based on a difference in solubility. It is believed that the proposed system offers possibilities for further development, such as miniaturisation and simplification, in the determination of sulphide.

4.6 References

[1] A. A. Ensafi, **Analytical Letters, 25**(1992)1525.

[2] K. Sonne and P. K. Dasgupta, **Analytical Chemistry, 63** (1991)427.

[3] V. Kubá P. K. Dasgupta and J. N. Marx, **Analytical Chemistry, 64** (1992)36.

[4] G. Bian, **Fenxi-Huaxue, 14** (1986)618.

[5] T. A. Arowolo, **Microchemistry journal, 45** (1992)97.

[6] X. Wang, **Fenxi-Huaxue, 15** 1987)21.

[7] M. O. Babiker and J. A. W. Dalziel, **Analytical Proceedings(London), 20** (1983) 609.

[8] P. Do-Nascrimento, S. Hinkamp and G Schwedt, **Vom-Wasser, 78** (1992)21.

[9] R. Bin-Ahmad, J. O. Hill and R. J. Magee, **Thermochimica Acta, 98** (1986)127.

[10] R. Narayanaswamy, F. Sevilla, **Analyst(London), 111** (1986)1085.

[11] J. F. Van Staden, **Analyst (London), 113** (1988)885.

[12] M. Yaqoob, L. Rishi, M. Masoom, **Journal Chem. Soc. Pakistan, 13** (1991)32.

[13] M. D. Luque de Castro, **Trends Anal. Chem., 11** (1992) 149.

[14] J. Martínez Calatayud and J. V. García Mateo, **Trends Anal. Chem., 12** (1993) 428.

[15] J. F. Van Staden. L. G. Kluever, **Anal. Chim. Acta, 350** (1997) 15.

[16] A. Sakuragawa, S. Nakayama, T. Okutani, **Analytical Sciences, 10** (1994)77.

[17] G. D. Marshall and J. F. van Staden, **Anal. Inst., 20** (1992) 79

CHAPTER 5

The determination of total iron in ground waters and multivitamin tablets using a solid-phase reactor with tiron immobilised on ion-exchange resin.

5.1 Introduction

The determination of iron in its various oxidation states has been studied for a variety of matrices and described in detail by numerous researchers [1 - 6]. Methods used include polarography [7], kinetic spectrophotometry [2,3,5], graphite furnace AAS [7], as well as flame AAS [8]. Because of the flexibility and ease of use offered by flow injection analysis, most of these classical techniques have been modified for use on flow systems [3,9 - 11].

An amount of work has also been done on speciation between the Fe(II) and Fe(III) oxidation states [12 - 14]. A paper by Kuroda *et al* [4] describes the determination of Fe(III) and total iron by first determining the iron(III) after complexing with tiron, then oxidising the iron(II) in the sample by UV irradiation and determining the total iron content. This was done by splitting the sample stream. In this fashion the Fe(II) in the sample could also be determined by simple subtraction. The reverse of this approach

was also used by Faizullah and Townshend [15] where they determined the iron(II) after complexing with 1,10-phenantroline, then reducing the iron(III) with a reducing column and determining the total iron content. As mentioned previously, the Fe(III)-content of a sample could be determined by subtraction. Another paper by Lynch *et al* [16] describes the use of different complexing agents in the same manifold for determining Fe(II) and Fe(III) simultaneously.

The aim of the work described in this paper was to find a simple method for determining Fe(III) in a sample without splitting and merging of sample zones and reagent streams. Because solid-phase reactors offer interesting and promising alternatives to methods normally used for analysis, particularly with regard to lowered reagent consumption and simplifying of FIA systems [17], modification of an existing method was attempted, for use in a system incorporating a solid-phase reactor.

This was attempted by immobilising the reagent (tiron) on a solid support material and placing a reactor filled with this reagent in the carrier stream. The structure is given in Figure 5.1. The sample was then simply pumped through the reactor and the iron(III) present reacted with the tiron in the solid phase.

Speciation was not attempted in this study as simplicity and quick analysis time were some of the main goals, as mentioned above. All the Fe(II) present in samples was chemically oxidised and the total iron determined as Fe(III).

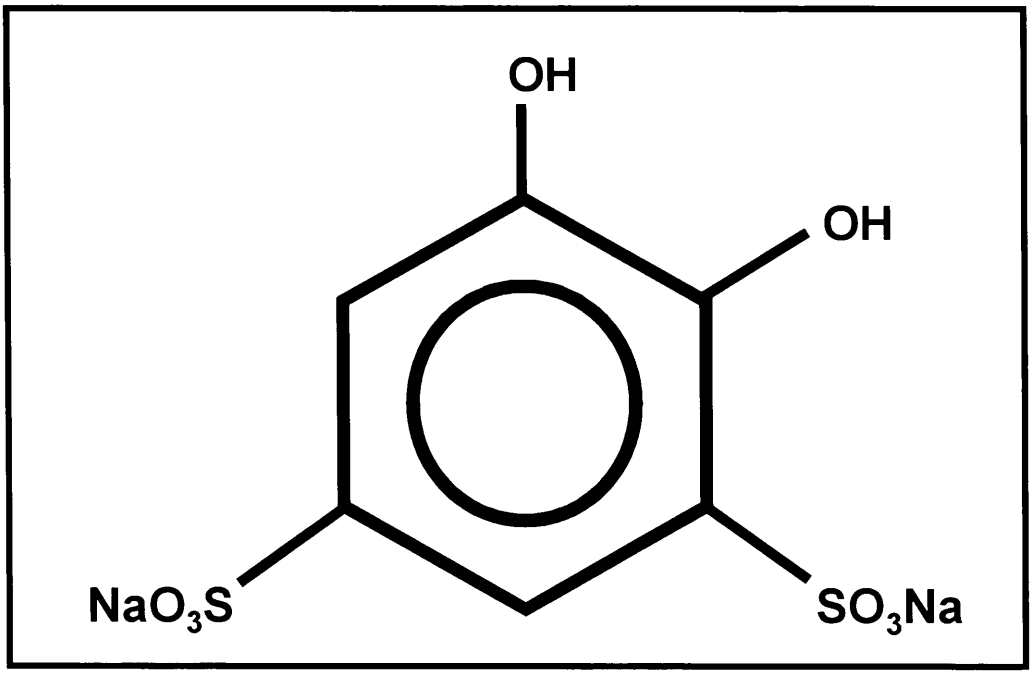

Figure 5.1: Structure of tiron

5.2 Experimental

5.2.1 Reagents and solutions

A standard solution containing 1000 mg ℓ^{-1} of iron(III) was prepared by weighing 7.382g of 98% pure iron(III)nitrate nonahydrate (Holpro Analytics), dissolving it in doubly deionised water and diluting to 1 litre. This solution was standardised with the aid of ICP-AES. Working solutions in the range 1 to 100 mg ℓ^{-1} were prepared by appropriate dilution of the standard solution with 0.07 mol ℓ^{-1} $HClO_4$ (Merck, Darmstadt).

The carrier stream was doubly deionised water from a MODULAB ModuPure water

purification system (Continental Water Systems International).

5.2.2 Instrumentation

The FIA system was constructed from the following components: a Cenco 24-channel peristaltic pump operating at 10 rpm, a VICI 10 Port 2-position sampling valve, a Unicam 8625 UV-Visible spectrophotometer equipped with a Hellma type flow-through cell (volume 80 $\mu\ell$) for absorbance measurements and a FlowTEK software package [18].

5.2.3 Operation of the system

The whole procedure, including data processing and storage was computer- controlled via *FlowTEK* using the same system as in chapter 4 [17]. The total analysis time for each sample was 85 seconds, of which the first five seconds were used to ensure the sample loop was filled, the next 45 seconds to inject the sample plug into the carrier stream, and the last 35 seconds to rinse the system and start filling the sample plug again. The injected Fe(III) reacted with the tiron in the reactor to form a blue complex with a maximum absorbtivity at 667 nm, which was determined spectrophotometrically.

5.2.4 The solid-phase reactor

The solid-phase reactor was constructed using Teflon tubing with an inner diameter of 1.52 mm. The reactor packing consists of Tiron (disodium1,2-dihidroxybenzene-3,5-

disulphonate) (BDH Chemicals, Poole, England) immobilised on Amberlite ion exchange resin (0.3-1.0 mm; BDH Chemicals, Poole, England). This packing was prepared by weighing 0.5 g Tiron in a beaker, adding 5 g Amberlite resin, as well as 50 mℓ deionised water, and evaporating the water over a period of 3 hours. The material was then dried in a drying oven at 70 °C for one hour.

Teflon tubing with a length of 9 cm and an inner diameter of 1.52 mm was used to construct a reactor. One end of the tube was stoppered with glass wool, and the solid-phase reagent prepared as above was introduced into the tube via a funnel, which was attached to a shaker. The reactor was then shaken for a minute to ensure close packing and the other end was also stoppered with glass wool.

The reactor was conditioned by pumping 30 injections of a 50 mg ℓ^{-1} Fe(III)-standard through it. This was done to ensure firstly the absence of air pockets and secondly repeatable behaviour of the reactor.

5.3 Method optimisation

The method was optimised with regard to the following parameters: flow speed, sample volume and acid content, transmission tube length and diameter, and reactor length and diameter. The relative peak height and %RSD were used (together) as criteria for establishing the optimum parameter value in each case.

5.3.1 SPR parameters

5.3.1.1 Reactor length

The solid-phase reactor (SPR) forms the crux of the system and a great deal of time was thus spent optimising the related parameters. The reactor length was varied between 50 and 100 mm, with the 90 mm reactor giving the largest response. Results are given in Table 5.1 and Figure 5.2.

The 50 mm reactor gave by far the best precision but this reactor became saturated much quicker than the other reactors, with a corresponding decrease in sensitivity, and was not used for further studies. The 90 mm reactor was used for further optimisation studies.

Table 5.1: Optimisation of reactor length

Reactor length (mm)	Peak height	% RSD
50	0.7551	0.57
60	0.7824	1.4
70	0.7991	1.2
80	0.8035	1.7
90	0.8540	1.3
100	0.8312	2.0

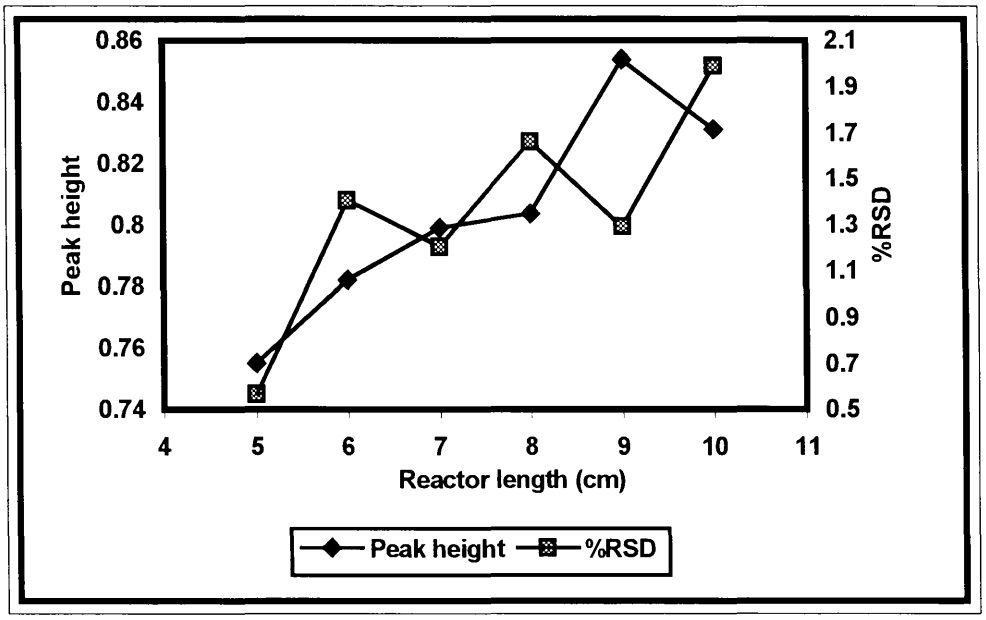

Figure 5.2: Optimisation of reactor length

5.3.1.2 Reactor inner diameter

The response of the reactor was also evaluated while varying the reactor inner diameter between 1.5 and 2.8 mm. Results are given in Table 5.2 and Figure 5.3. This particular optimisation study proved a bit troublesome, because a Teflon reactor was used for the optimisation of reactor length, but only one type of Teflon was available for diameter studies, namely that with an inner diameter of 1.5 mm. For other diameter reactors Tygon manifold tubing had to be used. These reactors were difficult to pack, because the packing material kept clinging to the wall of the tube. Even and tight packing of the reactors was thus not possible in every case. For this reason reactors with an inner diameter of smaller than 1.5 mm were not studied. Optimum results were obtained with this reactor of the smallest inner diameter.

Table 5.2: Optimisation of reactor inner diameter

Diameter (mm)	Peak height	% RSD
1.5	0.7959	0.31
2.1	0.8688	1.1
2.3	1.031	1.6
2.5	0.9491	1.4
2.8	0.2222	6.5

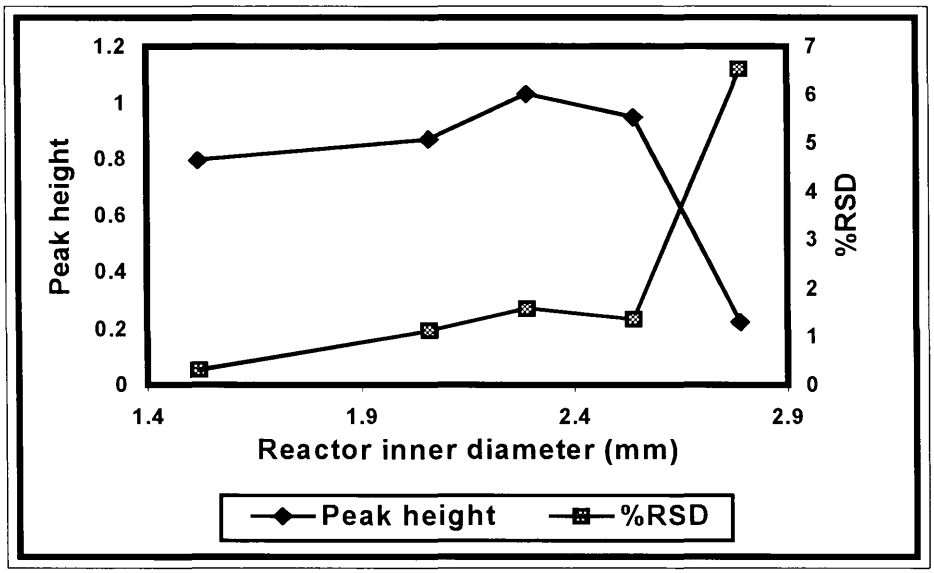

Figure 5.3: Optimisation of reactor inner diameter

5.3.2 Chemical parameters

5.3.2.1 Acid concentration of samples

The samples and standards were prepared in dilute $HClO_4$ and the specific concentration of the $HClO_4$ was optimised to determine the maximum sensitivity. Results are given in Table 5.3 and Figure 5.4.

Table 5.3: Optimisation of acid concentration in sample

$HClO_4$-concentration (mol ℓ^{-1})	Peak height	% RSD
0.01	0.08264	3.1
0.03	0.2876	1.4
0.05	0.4562	3.6
0.07	0.4521	2.3
0.09	0.4057	4.3

The concentration was varied between 0.01 and 0.09 mol ℓ^{-1}, with concentrations of 0.05 and 0.07 mol ℓ^{-1} giving the highest responses (relative peak heights of 0.4562 and 0.4521 respectively). The better precision was achieved with the concentration of 0.07 mol ℓ^{-1} $HClO_4$, and this parameter value was taken as the optimum.

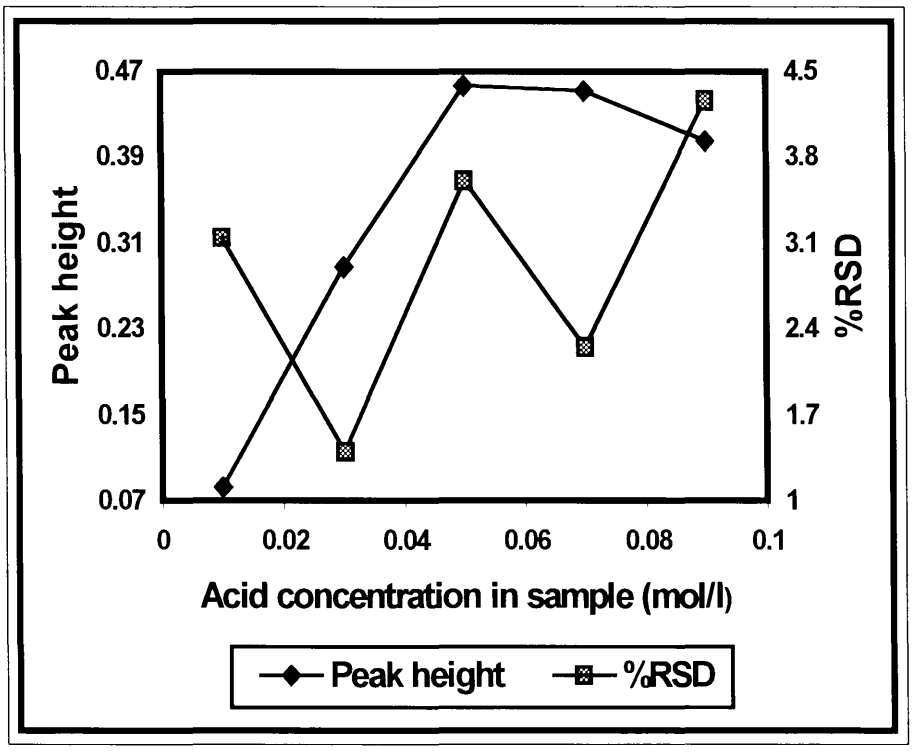

Figure 5.4: Optimisation of acid concentration

5.3.3 Physical parameters

5.3.3.1 Flow rate

As was the case with previous work done on solid-phase reactors [17], the optimum flow speed proved to be an intermediate value. Results are given in Table 5.4 and Figure 5.5.

Table 5.4: Optimisation of flow rate

Flow rate ($m\ell\ min^{-1}$)	Peak height	% RSD
0.60	0.3972	1.1
0.80	0.4224	2.7
1.0	0.4903	2.0
1.2	0.5010	2.0
1.4	0.5049	0.87
1.6	0.5005	0.74
2.0	0.4282	1.8

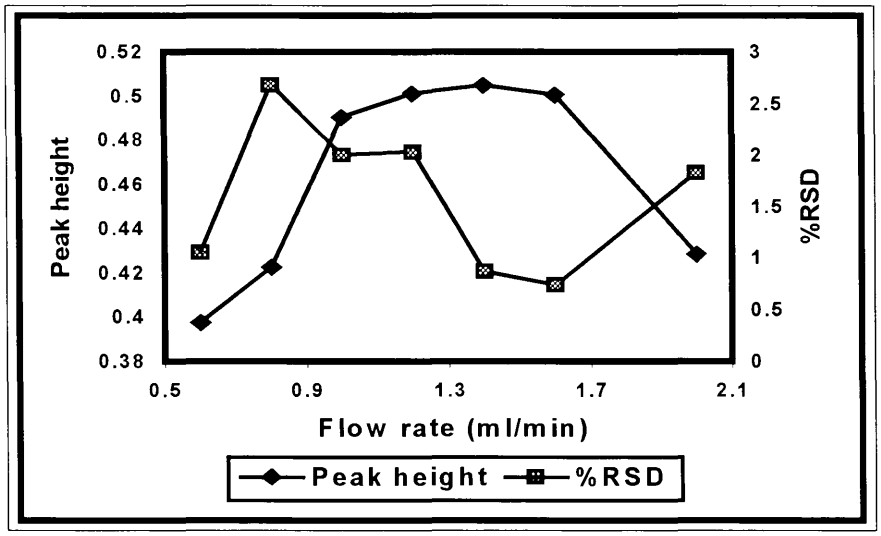

Figure 5.5: Optimisation of flow rate

The flow rate was varied between 0.60 and 2.00 $m\ell\ min^{-1}$, and the best results were achieved with speeds of 1.40 $m\ell\ min^{-1}$ and 1.60 $m\ell\ min^{-1}$. The latter flow rate was chosen as the optimum because of the lower % RSD achieved.

5.3.3.2 Sample volume

The effect of increasing sample volume was evaluated between 55 and 105 $\mu\ell$. Results are given in Table 5.5 and Figure 5.6.

Table 5.5: Optimisation of sample volume

Sample volume ($\mu\ell$)	Peak height	% RSD
55	0.3870	1.5
65	0.4480	1.7
75	0.4929	1.8
85	0.5751	2.0
95	0.6451	2.8
105	0.5660	3.4

Although the smallest sample volume gave the lowest % RSD, the relative peak height obtained was only 67 % of that obtained with a volume of 85 $\mu\ell$, while the %RSD was 74 % of the corresponding % RSD. A sample volume of 85 $\mu\ell$ was thus chosen as the optimum value.

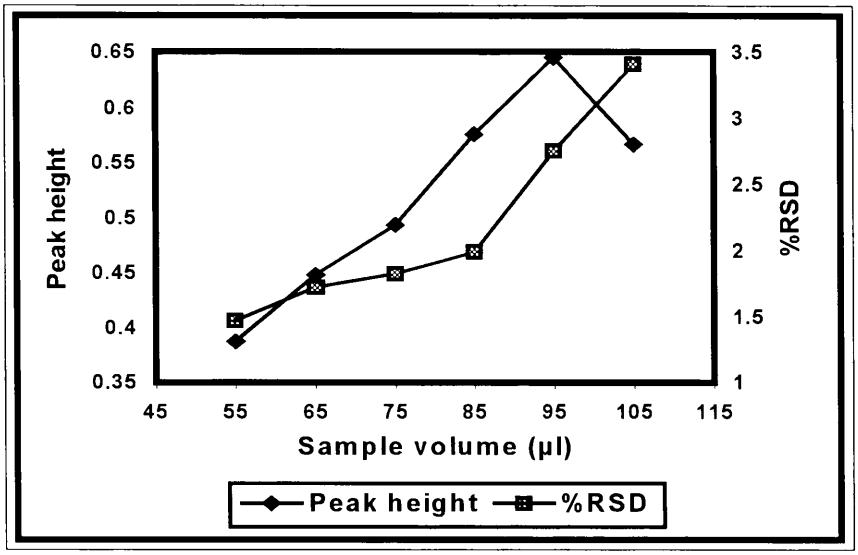

Figure 5.6: Optimisation of sample volume

5.3.3.3 Total tube length

The total tube length was varied between 46 and 56 cm. Results are given in Table 5.6 and Figure 5.7.

Table 5.6: Optimisation of total tube length

Tube length (cm)	Peak height	% RSD
46	0.4731	1.8
48	0.4883	2.7
50	0.4799	2.3
52	0.4883	1.4
54	0.4922	1.7
56	0.5527	3.5

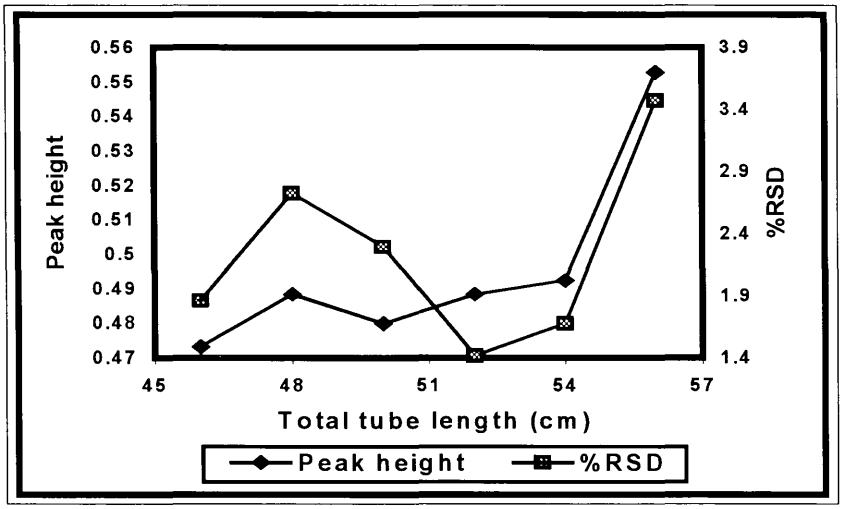

Figure 5.7: Optimisation of tube length

In contrast to previous work [17] the highest response was obtained with the longer tube (relative peak height: 0.5527), which would suggest that factors other than axial dispersion of the sample plug had an influence on the response. One factor could be that the reaction between the Fe(III)-ions in the sample and the tiron released from the reactor had not reached equilibrium by the time the sample plug reached the detector, which would point to slow reaction kinetics. Reproducibility however, decreased drastically with increasing tube length (% RSD for 56 cm reactor: 3.5), and an intermediate length of 52 cm was chosen for further studies because it gave an acceptable response and good reproducibility.

5.3.3.4 Tube internal diameter

Tube internal diameter was varied between 0.64 and 1.1 mm with the smallest diameter giving the best results. The relative peak height was 0.6923 and the RSD was 0.84 %. Results are given in Table 5.7 and Figure 5.8.

Table 5.7: Optimisation of tube internal diameter

Internal diameter (mm)	Peak height	% RSD
0.64	0.6923	0.84
0.76	0.6732	1.2
0.89	0.6030	1.7
1.0	0.5933	1.9
1.1	0.5030	2.9

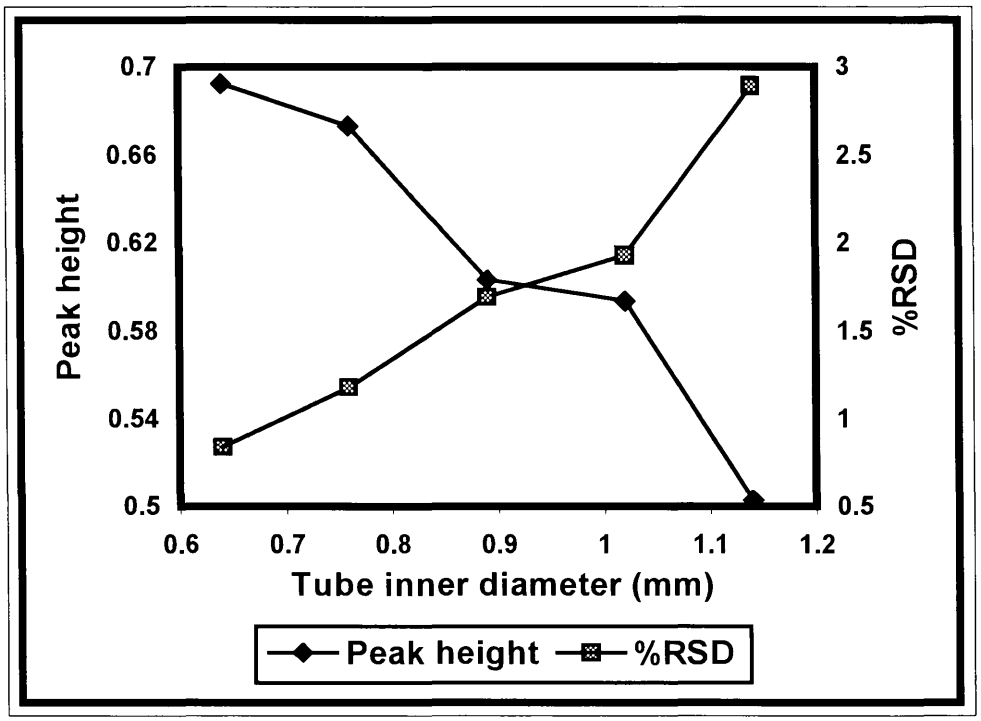

Figure 5.8: Optimisation of tube internal diameter

5.4 Method evaluation

The method was evaluated with regard to parameters such as linearity, sample interaction, accuracy, precision and interferences. The optimum conditions used are given in Table 5.8.

Table 5.8: Optimum values obtained and used for evaluation

Parameter	Optimum value
Reactor length	90 mm
Reactor inner diameter	1.5 mm
Acid concentration	0.07 mol ℓ^{-1}
Flow rate	1.60 mℓ min^{-1}
Sample volume	85 $\mu\ell$
Total tube length	52 cm
Tube inner diameter	0.64 mm

5.4.1 Linearity

The linearity of the method was evaluated under optimum conditions for analyte concentrations in the 1 to 100 mg ℓ^{-1} range. This was firstly done without electronic signal enhancement. The calibration curve is shown in Figure 5.9. The response of the system was linear for Fe(III)-concentrations in the range 1 to 50 mg ℓ^{-1}.

The relationship obtained between response and analyte concentration was:

$$y = 0.0566 + 0.0603x \qquad (5.1)$$

where y = relative peak height and x = Fe(III)-concentration (mg ℓ^{-1}). The correlation coefficient (r^2 = 0.999) indicated that the method is linear for Fe(III)-concentrations between 1 and 50 mg ℓ^{-1}.

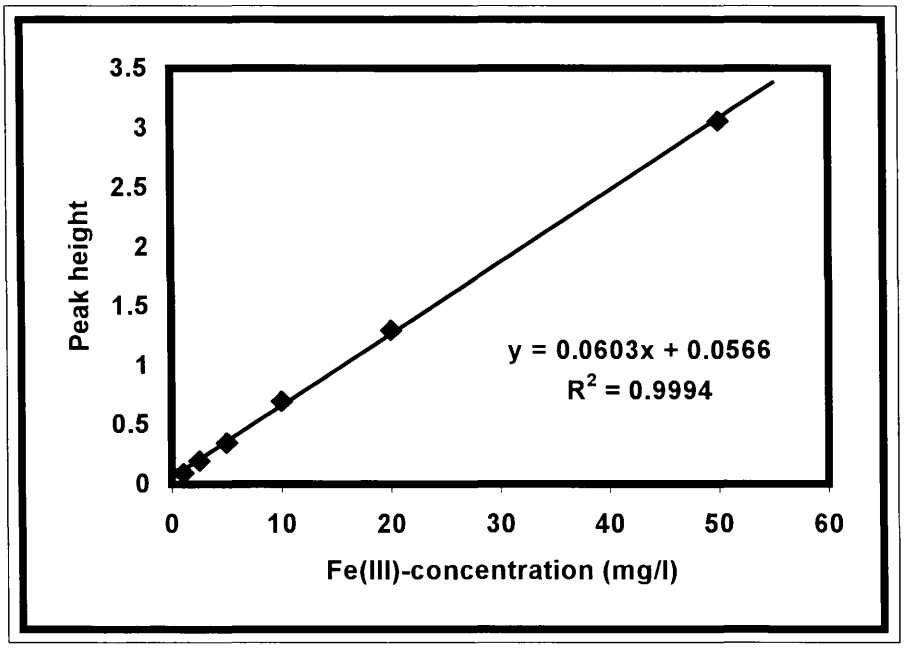

Figure 5.9: Calibration curve for Fe^{3+}

Although the linear fit applied to the data showed a good correlation between concentration and response, the method was still not sensitive enough. Increasing the sensitivity was attempted by electronically enhancing the signal from the detector. This yielded a calibration curve with a slope that was more than twice that obtained previously.

The relationship obtained between concentration and response was:

$$y = 0.1534 + 0.134x \; ; (r^2 = 0.999) \qquad (5.2)$$

with x and y denoting the same as previously mentioned.

The calibration curve is shown in Figure 5.10. As can be seen, the slope increased

more than twofold when compared to Figure 5.9 but the linear range was not increased substantially. This calibration curve was used for sample analysis because of the higher sensitivity.

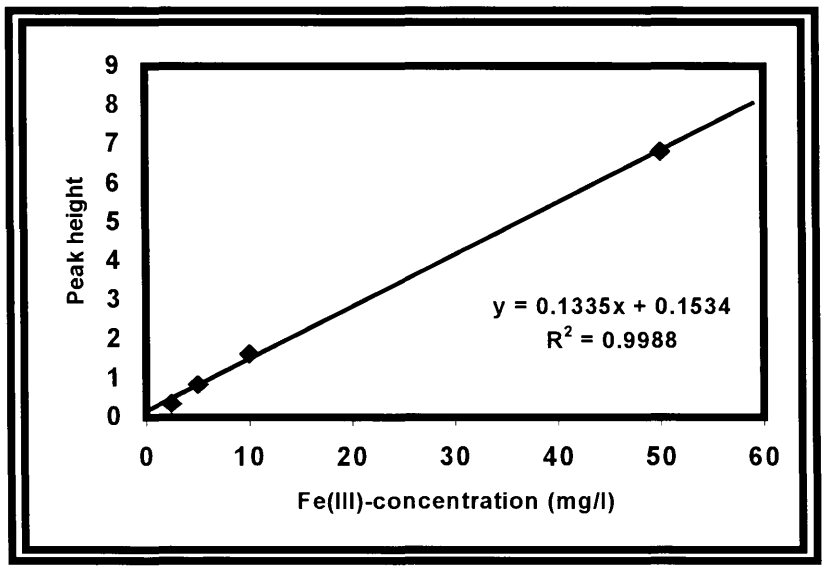

Figure 5.10: Calibration curve for Fe^{3+} with signal enhancement

5.4.2 Accuracy

Real samples (multivitamin tablets and ground water samples) of differing compositions were analysed with the method described in this chapter as well as a standard method. The tablets were dissolved in water (100 mℓ), 40 mℓ of 0.1 mol l^{-1} $K_2Cr_2O_7$ was added to oxidise all the Fe(II) to Fe(III) and the solution was diluted to 500 mℓ. The oxidising step was necessary because most of the iron in the tablets is found as Fe(II), and can not be detected with the proposed FIA-system.

The ground water samples were treated in a different way, because a lot of the iron

occurred in the form of a solid (probably Fe_2O_3), and this solid had to be dissolved. A 10 mℓ aliquot of the sample was pipetted into a glass beaker, 1.2 mℓ of concentrated $HClO_4$ added and the mixture was heated on a hotplate for 30 minutes, after which all the particulate matter was dissolved. The sample was then diluted to 100 mℓ in a volumetric flask and analysed.

Results are given in Table 5.9. As can be seen, the results obtained with the FIA-method were of the same order as those obtained with the standard method (ICP-AES).Both these sets of results compared well with the certified values.

Table 5.9: Comparison of results obtained by the proposed method with a standard method (ICP-AES)

Sample type	Certified Fe(III) (mg ℓ^{-1})	[Fe(III)] /mg ℓ^{-1} (proposed method)	[Fe(III)] /mg ℓ^{-1} (ICP-AES)
Multivitamin 1	6.30	6.05	6.48
Multivitamin 2	4.50	4.37	4.41
Ground water 1	-	27.5	29.1
Ground water 2	-	18.9	19.0
Ground water 3	-	35.3	35.6

5.4.3 Recovery

The recovery on the system was determined by spiking tap water samples with 1000 mg l^{-1} Fe(III), analysing and comparing the concentration obtained with an expected concentration, calculated with the aid of a calibration curve.

The equation used for determining the recovery was as follows:

$$\text{Recovery} = \frac{\text{experimental concentration of Fe(III)}}{\text{expected concentration of Fe(III)}} \times 100 \qquad (5.3)$$

In this case the expected concentration of Fe(III) in the tap water samples was 4.95 mg ℓ^{-1}, and the experimental values varied between 4.90 mg ℓ^{-1} and 5.05 mg ℓ^{-1}, giving values of between 99 % and 102 % for the calculated recovery on the system.

5.4.4 Precision

The precision of the method was determined by doing 12 repetitions of a standard solution as well as a sample under optimum conditions and calculating the % RSD for each solution. A low value for the % RSD was an indication of good precision and *vice versa*. The equation used for this calculation was:

$$\%\ \text{Relative standard deviation} = \frac{\text{standard deviation}}{\text{mean peak height}} \times 100 \qquad (5.4)$$

The standard deviation on the peak height of 0.8032 obtained with a 10 mg ℓ^{-1} Fe(III) standard was 6.9×10^{-3}, giving a % RSD of 0.86 %. The % RSD for an iron-rich ground water sample was calculated in the same way, with the standard deviation associated with the peak height of 2.68 being 2.7×10^{-2}. This gave an RSD of 1.0 % for the sample.

5.4.5 Sample interaction

The sample interaction was calculated by obtaining the peak height (relative response) for a 5 mg ℓ^{-1} standard followed by injection of volume of a 50 mg ℓ^{-1} standard and obtaining the peak height. The interacted signal was obtained directly after this by injection of the 5 mg ℓ^{-1} standard. These values for the peak heights were then substituted in the following equation

$$\text{Interaction} = \frac{A_3 - A_1}{A_2} \times 100 \qquad (5.5)$$

where A_1 = peak height (0.4736) of the uninteracted 5 mg ℓ^{-1} standard

A_2 = peak height (3.394) of the 50 mg ℓ^{-1} standard

and A_3 = peak height (0.4883) of the interacted 5 mg ℓ^{-1} standard.

The interaction calculated at a sampling rate of 45 per hour was between 0 % and 0.4 %, which is negligible.

5.4.6 Detection limit

The detection limit was calculated using the formula:

$$\text{Detection limit} = \frac{(3\sigma + K)(K - c)}{m} \qquad (5.6)$$

where σ is the relative standard deviation of the baseline, K is the average signal value

of the baseline and c and m are the intercept and slope of the calibration curve respectively.

The value obtained for the baseline signal was 0.0675 with a corresponding % RSD of 1.2. The values for the slope and intercept of the calibration curve was 0.0603 and 0.0566 respectively. These values gave a calculated detection limit 0.66 mg ℓ^{-1} when substituted into equation 5.3.

5.4.7 Interferences

The influence of various cations and anions on the method was investigated. Solutions with an Fe(III)-concentration of 10 mg ℓ^{-1} were spiked with interferents to determine the admissible concentration of interferent. The recovery was calculated referring to a 100% recovery of Fe(III) in the absence of interferents. The results are given in Tables 5.9 and 5.10. The Fe(III)-concentration was 10 mg ℓ^{-1} in each case.

Table 5.9: Summary of cation interferences
(with tolerable concentration given)

Ion	[Interferent] (mg ℓ^{-1})	%Recovery of Fe(III)
K	100	98.2
Na	100	97.3
Zn(II)	100	99.1
Ca(II)	100	99.4
Mg(II)	100	99.1
Cu(II)	100	102
Fe(II)	5	102

The only serious cation interferent encountered was the Fe(II) ion, but this was not a problem with the proposed method as all the iron present in the samples was oxidised to Fe(III) prior to analysis.

The most serious anion interference was caused by the carbonate ion. This ion caused no interference in the analysis of the ground water, but proved to be a problem in the analysis of effervescent multivitamin tablets.

Table 5.10: Summary of anion interferences

Ion	[Interferent] ($mg\,\ell^{-1}$)	%Recovery of Fe(III)
Cl^-	100	102
Br	100	100
SO_4^{2-}	100	98.5
NO_3^-	100	99.6
OH^-	100	95.2
CO_3^{2-}	100	86.2
CO_3^{2-}	100	87.1

5.5 Conclusion

The proposed method offers a promising alternative to previously used methods, with the advantages of having low reagent consumption and a simple system being important considerations. The method was highly accurate in determining total iron in ground water, but care should be taken when analysing effervescent tablets that contain large amounts of carbonate.

5.6 References

[1] S. M. Sultan and F. E. O. Suliman, **Analyst, 121** (1996) 617.

[2] S. N. Bhadani, M. Tiwari, A. Agrawal and C. S. Kawipurapu, **Mikrochim. Acta, 117** (1994) 15.

[3] R. Kuroda, T. Nara and K. Oguma, **Analyst, 113** (1988) 1557

[4] K. Oguma, S. Kozuka, K. Kitada and R. Kuroda, **Fresenius J Anal. Chem., 341** (1991) 545.

[5] J. Liu and H. Ma, **Talanta, 40** (1993) 969.

[6] T. P. Tougas, J. M. Janetti and W. G. Collier, **Anal. Chem., 57** (1985) 1377.

[7] H. S. Zhang, X. C. Yang and L. P. Wu, **Fenxi Huaxue, 24** (1996) 220.

[8] S. Blain and P.Treguer, **Anal. Chim. Acta, 308** (1995) 425.

[9] O. Abollino, M. Aceto, G. Sacchero, C. Sarzanini and E. Mentasti, **Anal. Chim. Acta, 305** (1995) 200.

[10] Y. L. Zhang, **Lihua-Jinyan, 30** (1994) 9-10, 14.

[11] J. M. Barrero, C. Camara, M. C. Perez-Conde, C. San-Jose and L Fernandez, **Analyst(London), 120** (1995) 431.

[12] R. M. Liu, D. J. Liu, G. H. Liu, A. L. Sun and Z. H. Zhang, **Fenxi Huaxue, 22** (1994) 1241.

[13] S. J. Cosano, M. D. Luque de Castro and M. Valcárcel, **J. Autom. Chem., 15** (1993) 147.

[14] S. J. Cosano, M. D. Luque de Castro and M. Valcárcel, **J. Autom. Chem, 15** (1993) 141.

[15] A.T. Faizullah and A. Townshend, **Anal. Chim. Acta, 167** (1985)225.

[16] T. P. Lynch, N. J. Kernoghan and J. N. Wilson, **Analyst, 109** (1984) 843.

[17] J. F. van Staden and L. G. Kluever, **Anal. Chim. Acta, 350** (1997) 15.

[18] G. D. Marshall and J. F. van Staden, **Anal. Inst., 20** (1992) 79.

CHAPTER 6

Final conclusions

When coming to the end of a piece of work one usually tries to evaluate the work according to certain objectives that were set at the start. In this study that was undertaken the most important aims were: lowered reagent consumption

system simplification

system miniaturisation.

When evaluating these objectives one has to consider the methods normally used for determining the analytes under discussion. In this case the methods used for comparison were flow injection methods, as most of the classic methods have been converted for use in flow systems.

6.1 Manganese method conclusion

For the determination of manganese(II) the popular FIA methods include those that are based on complexation with photometric detection [1] as well as those that make use of the catalytic effect of manganese on a compound that produces chemiluminescence [2].

The techniques most widely used however, are those that are based on atomic spectroscopy, whether it be absorption or emission [3,4]. In most cases, methods based on these techniques include preconcentration columns for trace determination, as discussed in chapter 2.

As the detectors for these methods require a lot of carrier gas (nitrogen or argon), and are usually relatively expensive to run it can be stated that the reagent consumption, and subsequently the running cost of the FIA system under consideration is lower than these spectroscopic methods. With regard to simplicity of the system, the method incorporating the solid-phase reactor makes use of only one stream that flows directly through the reactor and detector without splitting and is thus very simple and small. The method does not offer the large linear range or low detection limits achievable with spectroscopic techniques, though, which is partly due to the lack of a preconcentration step, but the simplicity and small size are important features that can not be ignored. In terms of the original aims of the project it can be said that these aims were achieved successfully.

6.2 Sulphide method conclusion

For the determination of sulphide with flow injection manifolds there are several standard methods regularly employed. These methods include determination by complexing with sodium nitroprusside as well as indirect determination by the formation of methylene blue from N,N dimethyl-p-phenylenediamine (DMPD) [5,6]. In both cases H_2S gas is evolved by acidification of the sample. The gas is then sent through a permeation unit where it

permeates into a basic carrier stream, which then merges with a stream containing the relevant reagents. In the nitroprusside method the product formed is $Na_4[Fe(CN)_5NOS]$ and this can be detected spectrophotometrically. In the methylene blue method the H_2S reacts with the DMPD after the latter has been oxidised by iron(II) present in the carrier stream. The reaction product is then methylene blue, which can also be determined spectrophotometrically. The manifolds for these two methods are rather complex, with a gas permeation unit as well as five streams and three junctions which allow for reagent addition and mixing. Compared to these two standard methods the proposed FIA system is relatively simple and small, with only two streams and a single sample injection point. The reagent consumption is also low when compared with the standard methods.

Another method of analysis regularly employed for the determination of sulphide makes use of ion-selective electrodes or ISE's [7]. These electrodes are constructed from silver foil, coated with silver sulphide, which is rolled into a tubular shape for use in a flow system. These electrodes perform very well in flow systems with regard to linearity, accuracy, detection limit and recovery, but they do have drawbacks with regard to baseline drift and conditioning times.

When comparing the method incorporating a solid-phase reactor with the ISE method the previous does not perform as well with regard to the above-mentioned parameters. With regard to the aims of the project the system size, simplicity and reagent consumption are not effectively improved.

6.3 Iron method conclusion

Of the three different methods using solid-phase reactors described in this thesis, the one used for the determination of iron was the most sensitive, precise and accurate. This method also had largest linear range of the three methods.

When surveying literature for flow injection methods for the determination of iron, one comes across a number of papers on the use of spectroscopic techniques like flame or graphite furnace AAS [8,9]. These methods usually determine the total iron content of a sample, because all the iron present is oxidised to the highest oxidation state in the flame or plasma. A number of papers deal with iron determination by complexometry and here a lot of work has been done on speciation between the iron(II) and iron(III) oxidation states [10,11]. Speciation is usually done by splitting the sample and delaying one part while the other part complexes with a suitable ligand, depending on the oxidation state, to determine the partial iron content. The remaining part is then oxidised or reduced and subsequently complexed with the same ligand to determine the total iron content. The usual ligand for complexation with iron(II) is 1,10-phenanthroline and that for complexation with iron is tiron or the thiocyanate ion. The complexes formed show absorbance maxima at certain wavelengths and the absorbance can be measured at these wavelengths. These methods usually show good precision (% RSD < 0.9) and recovery (> 95 %). As the proposed solid-phase method is effectively a modification of a homogenous method using tiron in the aqueous phase, it should prove worthwhile to compare these two methods with regard

to the aims mentioned at the start of the chapter. As the carrier stream for the homogenous method is acidic and that for the heterogeneous method is deionised water, one can see that there is already a reduction in reagents, namely perchloric or sulphuric acid. The amount of tiron used is also reduced, with only 0.5 g needed to prepare a batch of the immobilised reagent, compared to 1-3 g tiron used to prepare tiron solutions for homogenous methods. One batch of immobilised reagent can be used to construct a number of reactors, all of which can be used for 400 to 500 runs.

With regard to system simplification it can be said that the proposed system is once again simpler and smaller than the heterogeneous system under consideration, with only a single carrier stream and no splitting of the sample plug or merging points. The original aims of the study have thus been met to a large degree.

6.4 References

[1] T. Yamane and Y. Yamagushi, **Anal. Chim. Acta, 345** (1997) 139.

[2] A. Gaikwad, M. Silva and D. Perez-Bendito, **Anal. Chim. Acta, 302** (1995) 275.

[3] R. Ma and F. Adams, **Anal. Chim. Acta, 317** (1995) 215.

[4] X. Peng, Z. Juang and Y. Zeng, **Fenxi Huaxue, 21** (1993) 1410.

[5] V. Kubán, P. K. Dasgupta and J. N. Marx, **Anal. Chem., 64** (1992) 36.

[6] M. O. Babiker and J. A. W. Dalziel, **Anal. Proc., 20** (1983) 609.

[7] J. F. van Staden, **Analyst, 113** (1988) 885.

[8] H. S. Zhang, X. C. Yang and L. P. Wu, **Fenxi Huaxue, 24** (1996) 220.

[9] S. Blain and P. Treguer, **Anal. Chim. Acta, 308** (1995) 425.

[10] R. Kuroda, T. Nara and K. Oguma, **Analyst, 113** (1988) 1557.

[11] S. Abe, T. Saito and M. Suda, **Anal. Chim. Acta, 181** (1986) 203.